ORDER AND DISORDER IN SOME SURFACE
AND COLLOID SYSTEMS

PETER ALLAN FORSYTH Jr

A thesis submitted for the degree of

Master of Science

at The Australian National University,
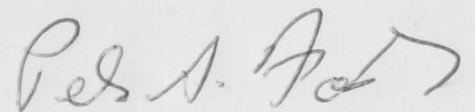
Canberra

January 1977

PREFACE

This thesis is an account of work carried out from September 1975 to January 1977 at the Department of Applied Mathematics, Research School of Physical Sciences, The Australian National University, for the degree of Master of Science.

During the course of this work I benefited immensely from discussions with many members of the Department. In particular I profited from Dr. S. Marčelja's remarks about non-equilibrium exchange rates, and was constantly elevated by Professor B.W. Ninham's example of absorption of amber colloidal systems. Of course I would like to thank my fellow students and friends for their continual assistance; without their help this work would have been completed far earlier!

I should also acknowledge the financial support I received in the form of an award under the Commonwealth Scholarship and Fellowship Plan.

To the best of my knowledge, no work previously written or published has been used in this thesis except where referenced in the text.

Peter A. Forsyth Jr

PUBLICATIONS

1. J.A. Blackburn, M.A.H. Nerenburg, P.A. Forsyth, Jr
    "Effect of phase-dependent conductivity on inductive weak links"
    J. Appl. Phys. 46 (1975) 5315-5316

2. M.A.H. Nerenburg, P.A. Forsyth, Jr, J.A. Blackburn
    "Excitation of cavity modes in rectangular Josephson junctions"
    J. Appl. Phys. 47 (1976) 4148-4150

3. P.A. Forsyth, Jr, S. Marčelja, D.J. Mitchell, B.W. Ninham
    "Onsager transition in hard plate fluid"
    J. Chem. Soc., Farad. Trans II 73 (1977) 84-88

4. P.A. Forsyth, Jr, S. Marčelja, D.J. Mitchell, B.W. Ninham
    "Stability of clay dispersions"
    Proc. of the International Society of Soil Science Conference on
    'Modification of Soil Structure', Adelaide, 1976 (in press)

5. P.A. Forsyth, Jr, S. Marčelja, D.J. Mitchell, B.W. Ninham
    "Electrostatically-induced phase transitions in charged lipid
    membranes"
    (in preparation)

ABSTRACT

This thesis examines the role of statistical mechanics in the theory of ordering of surface and colloid systems.

The first chapter gives a brief introduction to the traditional secondary minimum theory of ordered colloidal systems. Specific examples are discussed which show that this theory is not always applicable.

The second chapter is concerned with phase transitions in hard rod and hard disc fluids. The various parameters of the transition are calculated, and the results are discussed in relation to tobacco mosaic virus and clay dispersions. In the case of clay dispersions, qualitatively new results are predicted.

The third chapter gives a brief discussion of surface thermo-dynamics. The results of the third chapter are used in the fourth to determine the electrical "free energy" of a monolayer or bilayer consisting of two different types of lipids. Calculations show that electrostatics alone will not induce a phase separation. However, the results show that only a small specific interaction between lipids is required to produce such a separation.

The fifth chapter is concerned with the ordering of water near an interface. It is shown that in the case of aqueous non-electrolytes, it is possible to deduce an attractive solute-solute interaction from quite general assumptions. This solute-solute potential is calculated numerically. A specific example shows that these results agree with Monte Carlo calculations.

C O N T E N T S

CHAPTER 5. THE ORDERING OF WATER NEAR AN INTERFACE

CHAPTER 1

ORDERING IN COLLOIDAL SYSTEMS

1.1 INTRODUCTION

Traditionally, the ordering of colloid systems has been explained in terms of the DLVO theory [1,2]. This theory was developed to explain the stability of lyophobic colloids, and to this end it has had a great success. Since lyophobic colloids are not equilibrium states in the thermodynamic sense, the problem of the stability of colloidal dispersions is essentially one of kinetics. A case in point is the gold sol. If a gold crystal is brought into contact with water, it will never spontaneously disperse into a sol, and yet gold sols have been produced which are stable for many years. Thermodynamically, the gold crystal has a much lower free energy than the dispersion. The entropy gained in the creation of more kinetic units is very much less than the energy required to form the gold-water interface. Consequently, the crystal is the stable state.

Deryaguin and Landau [2], and Verwey and Overbeek [1] explained this stability by considering the total energy of interaction between two colloidal particles. By summing the van der Waals attraction and the double-layer repulsion, they were able to calculate the interaction energy curve as a function of particle separation. Using kinetic arguments, they showed that if the repulsive barrier is

much greater than $k_B T$, then the possibility of coagulation is extremely small, and hence for all practical purposes the sol can be considered "stable". Of course all such sols must eventually flocculate because of the large depth of the primary minimum (the energy of two particles in contact). However, when there is a large repulsive barrier, the time taken for appreciable flocculation may be many years [1].

Since the double-layer repulsion falls off exponentially while the van der Waals-London forces decrease as some power of the separation, there will be some point where the attractive force exceeds the repulsion. This will give rise to a secondary minimum in the potential energy curves. Verwey and Overbeek suggested that this secondary minimum should lead to a reversible long-range aggregation in contrast to the irreversible coagulation in the primary minimum [1,3]. Since the secondary minimum is usually smaller than $k_B T$ for small spherical particles, they expected this effect to be noticeable only for large spherical particles, or for highly anisotropic sols, i.e. thin plates and elongated rods. This theory has had some success in providing a qualitative explanation of the adherence of glass spheres to plates [4], and the appearance of "chains" of parallel gold platelets [5]. This theory also applies to Schiller layers [6], where the ordering of the layers is considered to result from the competition between the double-layer repulsion and gravity [7].

Of course, since colloidal dispersions consist of a large number of particles, they must obey the laws of statistical mechanics. This idea was succinctly put across in a recent article:

... a knowledge of the interaction free energy between two atoms or particles, taken in isolation, may tell us little of the properties

of an ensemble of such particles ... Thus the first moral to be learned from statistical mechanics is that the existence of a minimum in the two-particle interaction free energy in the associated or ordered state does not guarantee the formation of this state. Conversely, the existence of an associated or ordered state does not necessarily imply that the particles are sitting at a separation where there is a minimum in the two-particle interaction free energy. [8]

It is important to remember that the appearance of an ordered phase is determined from the conditions of equilibrium between an ordered phase *and a disordered phase*. In dilute solutions, where many-body effects can be ignored, the assumption of pairwise additivity of the interaction energies is a good approximation. If, in addition, the depth of the secondary minimum is much larger than k_BT, the increase in energy of the particles in the disordered phase must be compensated by a large gain in entropy. This can only be achieved if the disordered phase is extremely dilute. In this case the equilibrium between the two phases can safely be ignored, and the particles will undoubtedly sit very close to the secondary minimum [9]. However, in situations where many-body effects cannot be ignored, or where the depth of the secondary minimum is $\leqslant k_BT$, this procedure is not to be trusted!!

1.2 ORDERING IN LATEX SPHERE DISPERSIONS

It might be worthwhile at this point to consider a concrete example of a system where the secondary minimum theories break down, and where other theories have successfully explained the observed phenomena. Recently, it has become possible to produce monodisperse suspensions of spherical latex particles. If the volume fraction and salt

concentration are suitably adjusted, a phase separation is observed [10, 11,12]. The ordered phase is iridescent when the interparticle spacing is of the order of the wavelength of visible light, while the disordered phase appears milky white. The volume fraction vs. salt concentration phase diagram has been determined experimentally by visual observation of the iridescent phase [10].

From DLVO theory it is known that a decrease in electrolyte concentration will decrease the depth of the secondary minimum. Consequently, if the phase separation of the latex spheres is caused by aggregation into the secondary minimum, a decrease in the salt concentration should result in a dissolution of the ordered phase. In fact, the opposite effect is observed — decreasing the electrolyte concentration results in increased ordering [10]. Since van der Waals forces are negligible at the large interparticle spacing in the ordered phase, the ordering must be determined largely by repulsive electrostatic forces [13].

There have been several attempts at a theoretical explanation of this phenomenon. It was apparent from the previous considerations that it was necessary to consider the statistical mechanics of the system. Using the well known pair potential for spherical colloidal particles (i.e. the sum of van der Waals and double-layer forces) the various thermodynamic quantities of interest were determined from Monte Carlo calculations [14]. The results were in qualitative agreement with experimental data. However, because of the small number of molecules used in the calculation, it was not possible to reproduce a coexistence region.

The latex system can also be modelled as a collection of hard

spheres. The effective radius of these spheres is taken to be one-half of the interparticle distance at which the interaction energy exceeds some small multiple of $k_B T$ [15]. It is well known from computer experiments that hard spheres will undergo a liquid-solid phase transition between volume fractions .5 - .55 [16]. Using this result and an effective volume determined by the double-layer repulsion, the real volume fraction vs. salt concentration phase diagram was calculated from the hard sphere model. The results compared favourably with the Monte Carlo calculations [15].

The hard sphere model was also compared directly with the experimental data, with good qualitative agreement [17], although the coexistence region appeared to be too narrow. This could be the result of experimental error, or the neglect of attractive forces which would tend to widen the coexistence region.

The hard sphere model is probably an excellent description of the transition for large volume fractions and high salt concentrations, where the electric field is highly screened. However, at low salt concentrations many-body effects will become important. Also, the expressions used for the interaction free energy of two colloidal particles assume that the particles are in equilibrium with bulk electrolyte. In solutions containing small amounts of salt, the diffuse double layers of the particles fill up the entire volume of the system, and there is no place to be regarded as "bulk".

A remedy to these difficulties was sought in the form of a Wigner lattice model of the latex system [13]. Here, each particle is considered to move about in a sphere containing equal and opposite charge centred on the lattice site. The many-body effects are taken

into account in an approximate way by requiring that the counterions be
localized in a Wigner-Seitz cell associated with each individual latex
particle. This is different from the usual treatment where the counter-
ions are regarded as being dispersed in the bulk region. By comparison
with the numerical simulation of the Wigner transition [18] (fluid-solid
transition of particles interacting via Coulomb forces) the authors were
able to compute the phase diagram of the system. At volume fractions
less than .2, the agreement with experimental data was quite good.
However, because of the nature of the model used (1/r Coulomb potential)
the coexistence region is extremely narrow.

The example of the latex spheres shows clearly that the DLVO
secondary minimum theory of ordering should not be regarded as a
panacea. Although the theoretical models differ in many respects, they
all require the use of statistical mechanics and the consideration of
phase equilibria.

REFERENCES – CHAPTER 1

[1]   E.J.W. Verwey and J.Th.G. Overbeek, *Theory of the Stability of Lyophobic Colloids* (Elsevier, Amsterdam: 1948).

[2]   B. Deryaguin and L. Landau, *Acta Physiochimica URSS* <u>14</u> (1941) 633.

[3]   J.Th.G. Overbeek, in *Colloid Science* (ed. H.R. Kruyt), Vol. I, Chap. 8 (Elsevier, Amsterdam: 1952).

[4]   A. von Buzagh, *Kolloid-Z.* <u>47</u> (1929) 370.

      A. von Buzagh, *Kolloid-Z.* <u>51</u> (1930) 105.

[5]   S. Okamoto and S. Hachisu, *J. Coll. Interface Sci.* <u>51</u> (1930) 105.

[6]   P. Bergman, P. Löw-Beer and H. Zocher, *Z. Phys. Chem.* A<u>181</u> (1938) 301.

[7]   K. Furusawa and S. Hachisu, *J. Coll. Interface Sci.* <u>28</u> (1968) 167.

[8]   J.N. Israelachvili and B.W. Ninham, *J. Coll. Interface Sci.* (in press).

[9]   I.F. Efremov, in *Surface and Colloid Science* (ed. E. Matijević), Vol. VIII, Chap. 2 (Wiley-Interscience: 1976), and the works cited therein.

[10] S. Hachisu and Y. Kobayashi, *J. Coll. Interface Sci.* <u>42</u> (1973) 342.

[11] A. Kose, M. Ozaki, K. Takan, Y. Kobayashi and S. Hachisu, *J. Coll. Interface Sci.* <u>44</u> (1973) 350.

[12] J.C. Brown, P.N. Pussey, J.W. Goodwin and R.H. Ottewill, *J. Phys.* A <u>8</u> (1975) 664.

[13] S. Marčelja, D.J. Mitchell and B.W. Ninham, *Chem. Phys. Letts.* <u>43</u> (1976) 353.

[14] I. Snook and W. van Megen, *Chem. Phys. Letts.* <u>33</u> (1975) 156.

[15] W. van Megen and I. Snook, *Chem. Phys. Letts.* <u>35</u> (1975) 399.

[16] B.J. Alder and T.E. Wainwright, *Phys. Rev.* <u>127</u> (1962) 359.

[17] S.L. Brenner, *J. Phys. Chem.* <u>80</u> (1976) 1473.

[18] C.M. Care and N.H. March, *Adv. Phys.* <u>24</u> (1975) 101.

CHAPTER 2

ORDERING IN TOBACCO MOSAIC VIRUS AND CLAY DISPERSIONS

2.1 TOBACCO MOSAIC VIRUS

Perhaps one of the more interesting colloidal dispersions of anisotropic particles consists of tobacco mosaic virus (TMV). The individual virus particles are rod-shaped with a length of approximately 2800 Å and a diameter of 180 Å. Very dilute (less than 3% by weight) aqueous solutions of TMV separate into two phases with a narrow coexistence region [1]. The top layer is isotropic while the bottom layer exhibits spontaneous birefringence. This indicates of course that the TMV "lines up" in the ordered phase. In some cases a third phase, an iridescent gel, will separate from the bottom layer [1]. Many other biological structures appear to form an ordered array of long proteins [2,3,4], and consequently TMV seems to be a good example of such systems.

If the behaviour of TMV is explained by a secondary minimum theory, then it is expected that the addition of salt will promote ordering, vis-à-vis the latex spheres. However, if electrolyte is added to the two-phase TMV system, the volume of the ordered phase decreases and eventually disappears altogether [1]. This would seem to indicate that secondary minimum theories are inapplicable.

The equilibrium gels observed by Bernal and Fankuchen [5] are

clearly the dense phase of a two-phase system, since the separation of the particles in this phase is determined solely by the properties of the solvent, and is independent of the amount of solvent present [5].

Many authors [6] have tried to explain the observed X-ray spacings by a force balance argument assuming that the van der Waals force balances the electric double-layer repulsion. These arguments have recently been reanalysed using new experimental data [7]. It appears that the observed spacings are always greater than those calculated from force balance, and that the salt dependence of the particle separation cannot be explained by shifts in the "equilibrium position". In any case, the depth of the energy well is merely of the order of $k_B T$. Consequently it is clear that attractive forces will not strongly affect the ordering of TMV, and that the spacing of the particles is determined to a large extent from the conditions of phase equilibrium.

2.2 CLAYS

Natural clays consist of roughly disc-shaped plates about 20 Å thick and with diameters ranging from 500 Å to 10,000 Å. The fractions of relatively uniform size can be separated after centrifugation [8].

In 1938, I. Langmuir and U.J. Schaeffer studied the properties of dilute dispersions of California bentonite [9]. Examination of the clay sol between crossed polaroids revealed two distinct phases. Solutions of less than 2% concentration (by weight) formed an isotropic phase, while those of more than 2.2% were birefringent. In the range 2 - 2.2% the two phases separated after standing for several hundred

hours. Apparently the properties of the anisotropic phase, as well as the corresponding phase transition, have never been closely examined.

As with the TMV, the particles in the ordered phase must have a preferred orientation. Since the clay particles are highly irregular in shape, it is unlikely that they form a periodic crystal lattice. This contention is supported by the observation that birefringence in bentonite sols is not associated with mechanical strength [9]. Instead, the experiments seem to indicate orientational order without a periodic structure, typical of nematic liquid crystals. Since the clay plates are very thin, and the interparticle spacings in dilute solutions are very large ($\sim 10^3$ Å), the van der Waals energy is negligible compared with the thermal energy.

2.3 THE ONSAGER TRANSITION IN HARD DISC AND HARD ROD FLUIDS

The physical basis for understanding the behaviour of colloidal suspensions of anisotropic particles has been described in the classic work of Onsager [10]. Colloidal particles interacting through the electrical double layer may be modelled by hard rods or hard discs. With the correspondence between the two systems established, Onsager has formulated the statistical mechanics of the problem within the second virial approximation, shown to be valid for highly anisotropic particles. With increasing concentration, both hard rods and hard discs show a transition from an isotropic fluid to a nematic fluid. Following previous work, this transition will be referred to as the Onsager transition.

Since Onsager's work, numerous investigations have confirmed the validity of his theory for systems of hard rods [11]. However, the hard disc fluid, which is the simplest theoretical model system of clay dispersions, has been neglected.

At first sight, it is difficult to see how a phase transition can take place in systems interacting only through repulsive (hard core) forces, i.e. for entropic reasons only. However, it is possible to make some qualitative arguments for the existence of two phases in a fluid of hard rods. (The same arguments apply to hard disc fluids, but for convenience only rods will be discussed in the following.)

If the concentration of a dilute system of hard rods is increased, it is clear that the rods will experience a loss in entropy, since they are no longer completely free to rotate. However, if some of the rods become oriented in a single direction, they are more efficiently packed than rods of random orientation. Thus the ordered rods will form a dense phase. The remaining particles will now have a greater freedom, and hence the disordered phase will gain in entropy. At some point the gain of entropy in the disordered phase will outweigh the loss of entropy in the ordered phase, and the system will spontaneously separate into two phases.

The following brief description of the Onsager theory will be restricted to the hard disc fluid — the modifications for hard rods are trivial.

The orientation of a disc can be described by specifying the angle between the normal to the disc and the preferred axis. If $\rho(\Omega)$ is the number of particles per unit volume having orientation in the solid

angle Ω to $\Omega + d\Omega$, then the probability distribution function $f(\Omega)$ is defined by:

$$\rho(\Omega) = \rho_0 \, f(\Omega) \, d\Omega \, ,$$

where ρ_0 is the total number density. In the case of random orientation, i.e. in the isotropic phase, $f(\Omega) = 1/4\pi$. The free energy of a fluid of hard rods or hard discs is given as a series expansion in the distribution function, viz. [10]:

$$
\frac{F}{Nk_B T} = \mu_0(T) + \log \rho_0 + \int f(\Omega) \, \log[4\pi f(\Omega)] \, d\Omega
$$

$$
+ \frac{\rho_0}{2} \iint \beta_1(\Omega,\Omega') \, f(\Omega) \, f(\Omega') \, d\Omega \, d\Omega'
$$

$$
+ \frac{\rho_0^2}{3} \iiint \beta_2(\Omega,\Omega',\Omega'') \, f(\Omega) \, f(\Omega') \, f(\Omega'') \, d\Omega \, d\Omega' \, d\Omega'' + \ldots \quad (2.3.1)
$$

Here $\mu_0(T)$ is a function of temperature only and represents the kinetic energy of the discs. $\beta_1(\Omega,\Omega')$ is the "excluded volume" of two discs of respective orientation Ω,Ω'. Similarly $\beta_2(\Omega,\Omega',\Omega'')$ represents the probability that three particles of orientations Ω,Ω',Ω'' will overlap simultaneously.

For low density dispersions, three-particle overlap is much less probable than two-particle collision. Higher order terms in the expansion contain higher powers of ρ_0, as well as the factors $\beta_2(\Omega,\Omega',\Omega'')$, $\beta_3(\Omega,\Omega',\Omega'',\Omega''')$, ... which are smaller than $\beta_1(\Omega,\Omega')$. Eqn (2.3.1) is therefore approximated by:

$$
\frac{F}{Nk_B T} = \mu_0(T) + \log \rho_0 + \int f(\Omega) \, \log[4\pi f(\Omega)] \, d\Omega
$$

$$
+ \frac{\rho_0}{2} \iint \beta_1(\Omega,\Omega') \, f(\Omega) \, f(\Omega') \, d\Omega \, d\Omega' \, . \quad (2.3.2)
$$

The first two terms in Eqn (2.3.2) represent the free energy of an ideal

gas, while the next two terms are corrections due to the finite size of the anisotropic particles. The third term represents an "orientational entropy" which is minimized by random orientation, while the fourth term is an "entropy of packing" which is minimized by perfect ordering [12]. Since all calculations are independent of $\mu_0(T)$, the precise form of this term is irrelevant. For particles of thickness (length) l and diameter d, $\beta_1(\Omega,\Omega')$ is given by [10]:

$$\beta_1(\Omega,\Omega') = \frac{\pi}{2} d^3 \sin\gamma + \frac{\pi}{2} l d^2 + \frac{\pi}{2} l d^2 |\cos\gamma|$$

$$+ 2l d^2 E(\sin\gamma) + 2l^2 d \sin\gamma . \qquad (2.3.3)$$

Here γ is the angle between the normals to the two discs, and $E(\sin\gamma)$ is the complete elliptic integral of the second kind.

Some rough estimates of the errors incurred by truncating the virial expansion were made in the original article [10]. While the errors can be shown to be small for thin rods [13], it is not possible to make rigorous estimates of the error in the case of discs. Nevertheless it is expected that these errors will be small, and that the results will be at least qualitatively correct.

If the anisotropic phase has cylindrical symmetry about the preferred axis, then $f(\Omega)$ may be expanded in a series of Legendre polynomials. Furthermore, since θ and $-\theta$ describe the same orientation, i.e. $f(\cos\theta) = f(-\cos\theta)$, then the expansion contains only even orders of Legendre polynomials, viz.:

$$f(\Omega) = \frac{1}{4\pi} \left\{ 1 + \sum_{i=2,4,6,\ldots} a_i P_i(\cos\theta) \right\} . \qquad (2.3.4)$$

In this form the distribution function satisfies the normalization

condition:

$$\int f(\Omega) \; d\Omega = 1 \; .$$

If the expansion for $f(\Omega)$ is substituted into Eqn (2.3.2), then the a_i can be determined by minimizing the free energy. The expansion for $f(\Omega)$ was truncated after the first seven non-vanishing terms ($i \leqslant 14$) and the coefficients were determined by using a numerical optimization method [14] to minimize Eqn (2.3.2). In the isotropic phase, of course, the a_i are identically zero, and $f(\Omega) = 1/4\pi$. For a given value of l/d, the transition densities were determined by equating the chemical potentials and pressures of both phases. This procedure is described in Appendix 1. Note that the use of a "hard" potential results in transition densities which are independent of temperature.

Colloidal particles are not "hard" in the conventional sense, but interact through the electrical double layer. The range of the electrostatic repulsion is determined by the ambient electrolyte concentration. If the plate diameter is much larger than the Debye screening length, we can regard the double layer repulsion as an additive short-range force. In terms of the hard fluid model, this short-range force will increase the effective size of the particles.

We define the anisotropy ratio x as a ratio of the smallest to the largest dimension for either rods or plates (i.e. for rods $x = d/l$, plates have $x = l/d$). Isotropic particles will have $x = 1$, while completely anisitropic particles have $x = 0$. If the salt concentration is increased, the range of the electrostatic force will be decreased, and hence the particles will become more anisotropic. Thus, increasing the salt concentration corresponds to decreasing x.

15

In Fig. 2.1, the transition concentrations are plotted for both rods and plates as a function of the anisotropy ratio x. It is immediately clear that the behaviour of plates differs markedly from that of rods. When $x = 0$, the transition concentration c_t of rods is infinite, while for thin plates, c_t is finite. As x increases, c_t for rods *decreases*, while c_t for plates *increases*.

The physical basis for this behaviour can be understood from an examination of Eqn (2.3.3), which gives the excluded volume of anisotropic particles. Plates of infinitesimal thickness have a non-zero excluded volume, while rods of vanishing diameter have zero excluded volume. Since a fluid of one-dimensional rods has zero probability of intersection, c_t at $x = 0$ is infinite. Consequently any increase of the diameter (increasing x) will lower c_t to some finite value. Thus we expect, at least initially, that c_t will decrease as x increases. However, this trend cannot continue indefinitely. Since the Onsager transition is a result of the anisotropy of the particles, c_t should at some point begin to increase with x. (Completely isotropic particles will not undergo an Onsager transition.) However, at $x = .2$, the volume fraction of the rods exceeds 100%, and c_t is still decreasing, albeit quite slowly. Of course, at high concentrations the truncation of the virial expansion in Eqn (2.3.2) is inaccurate. Consequently, over the entire range of concentrations where Eqn (2.3.2) is valid, the increase of the volume of the rods dominates the effect of decreasing anisotropy and thus c_t always decreases as x increases. In terms of salt concentration, we see that for rod-like particles increasing the electrolyte concentration (decreasing x) causes c_t to increase. This phenomenon is observed in solutions of tobacco mosaic virus [1]. How-
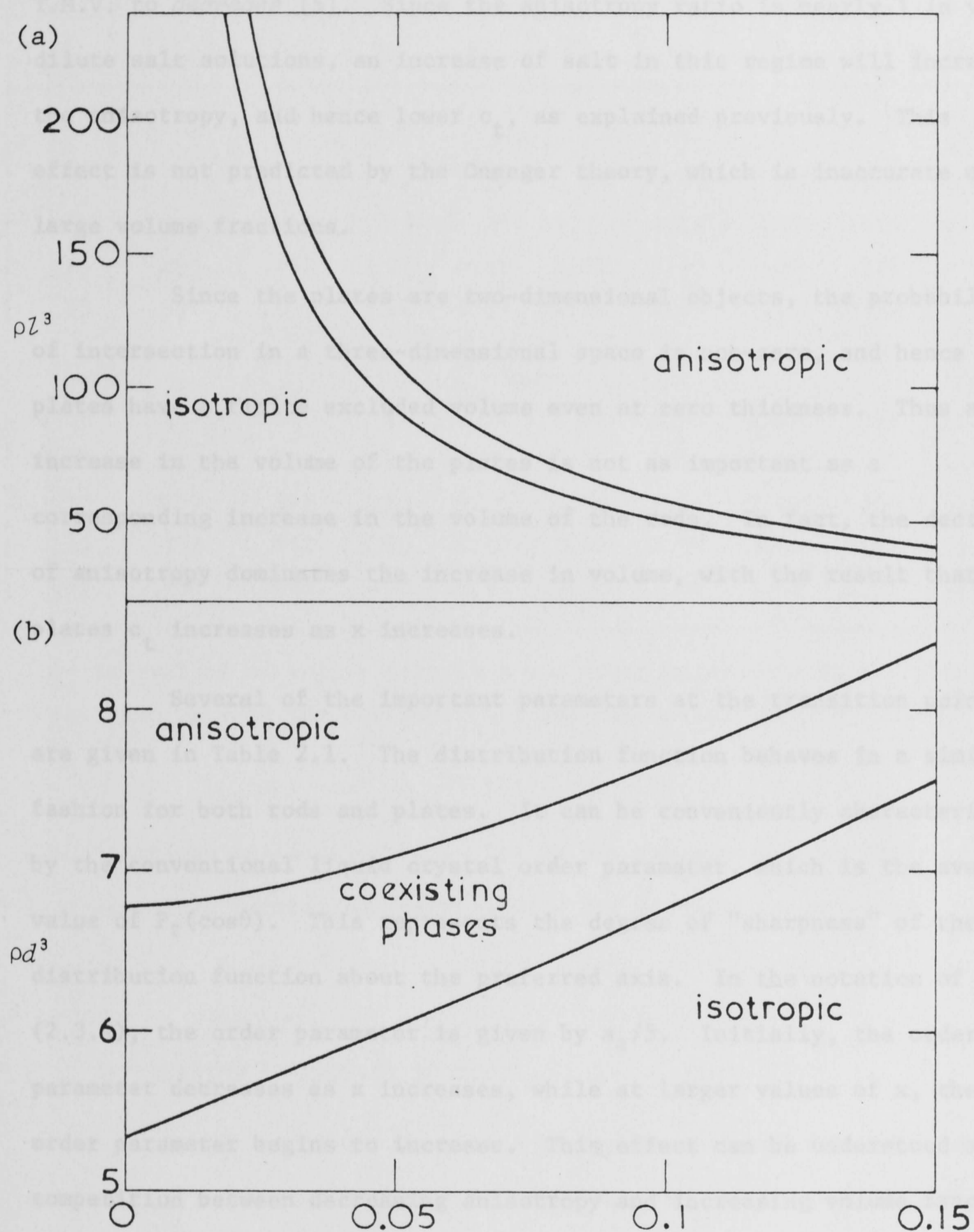
Fig. 2.1. Density of hard rod (a) or hard plate (b) dispersions at the Onsager phase transition as a function of the anisotropy ratio x. Increase of electrolyte concentration corresponds to a decrease in the value of x.

ever, in *very* dilute salt solutions, the addition of salt causes c_t of

T.M.V. to *decrease* [5]. Since the anisotropy ratio is nearly 1 in very

dilute salt solutions, an increase of salt in this regime will increase

the anisotropy, and hence lower c_t, as explained previously. This

effect is not predicted by the Onsager theory, which is inaccurate at

large volume fractions.

Since the plates are two-dimensional objects, the probability

of intersection in a three-dimensional space is non-zero, and hence the

plates have a finite excluded volume even at zero thickness. Thus an

increase in the volume of the plates is not as important as a

corresponding increase in the volume of the rods. In fact, the decrease

of anisotropy dominates the increase in volume, with the result that for

plates c_t increases as x increases.

Several of the important parameters at the transition points

are given in Table 2.1. The distribution function behaves in a similar

fashion for both rods and plates. It can be conveniently characterized

by the conventional liquid crystal order parameter, which is the average

value of $P_2(\cos\theta)$. This represents the degree of "sharpness" of the

distribution function about the preferred axis. In the notation of Eqn

(2.3.4), the order parameter is given by $a_2/5$. Initially, the order

parameter decreases as x increases, while at larger values of x, the

order parameter begins to increase. This effect can be understood as a

competition between decreasing anisotropy and increasing volume fraction.

The former dominates at small x, while the latter dominates at large x.

In any case, this effect is very small, and since the volume fraction at

which the order parameter begins to increase (30% for plates, 45% for

rods) is relatively large, the validity of Eqn (2.3.2) at these

Table 2.1

x	$V_0\rho_A$	$V_0\rho_I$	a_2	a_4	a_6	a_8	a_{10}	a_{12}	a_{14}
					Plates				
0	0	0	3.94	4.54	3.62	2.34	1.28	.573	.164
.05	.279	.237	3.83	4.30	3.35	2.12	1.15	.516	.151
.10	.605	.532	3.87	4.47	3.62	2.40	1.36	.629	.191
.15	.994	.891	3.98	4.87	4.21	2.98	1.79	.870	.275
					Rods				
0	-	-	3.94	4.54	3.62	2.34	1.28	.573	.164
.05	.216	.182	3.84	4.31	3.35	2.12	1.15	.510	.149
.10	.457	.397	3.83	4.36	3.46	2.24	1.24	.564	.168
.15	.753	.652	3.90	4.60	3.80	2.58	1.49	.701	.216
.20	1.050	.947	4.00	4.93	4.30	3.08	1.86	.912	.290

The values of volume fractions and order parameters at the phase transition between the isotropic (I) and the anisotropic (A) phase. concentrations is questionable. The volume fraction of the transition is a monotonic increasing function of x for either rods or plates.

2.4 APPLICATION OF RESULTS TO T.M.V.

Since the observed transition concentrations of T.M.V. are very low [1], the inter-particle spacing must be large and hence the van der Waals forces weak. To a sufficient approximation the particles interact solely through the electric double layer. If the salt concentration is large enough so that the double layer is confined to a region small compared with the rod length, then the effect of the double

layer is merely to increase the "effective diameter" of the rod. This effective diameter can be determined from the separation at which the double layer energy exceeds some small multiple of the thermal energy $k_B T$ [10]. Typically this will be of the order of $1/\kappa$, the Debye screening length. Consequently, the T.M.V. system can be replaced by a model fluid of hard rods; the length of the rods is the actual physical length of the T.M.V., while the diameter is now an "apparent" diameter determined by the range of the electric field.

The concentration of the disordered phase in the coexistence region was observed to be 2.3% by weight [1]. Unfortunately the salt concentration and pH of the bathing solution were not reported. As a result, it is not possible to estimate the effective diameter from energy considerations. A similar calculation to the one presented in Section 2.3 has been given previously for the case of spherocylinders — rods with hemispherical caps [12]. Of course for long rods (x small) the results are similar to Fig. 2.1. (It must be noted that in ref. 12 ρv_0 is plotted vs. x, while of course in the physical situation of changing salt concentration, the apparent volume of the rods v_0 is not a constant. The author attempted to compare his calculations with the experimental data on T.M.V. using an arbitrarily chosen effective diameter of 500 Å. Not surprisingly the agreement was poor.)

It is clear from Fig. 2.1 that the addition of salt (decreasing x) results in an increasing transition concentration as is observed in T.M.V. If the molecular weight of T.M.V. is taken to be 4×10^7, with a length of 2800 Å, then the experimental value of $\rho_t \ell^3$ (the dimensionless transition concentration) in the disordered phase is 7.6 [1]. The lowest value obtained from Table 2.1 is ~ 30.1

$(\rho l^3 = 4/\pi \rho v_0 \, x^{-2})$ for $x = .2$. As noted previously, at this value of x, the volume fraction of hard rods in the ordered phase exceeds 100%; obviously the Onsager theory is no longer valid for such large values of x. Since the solvent was reported as "aqueous solution" [1], it is likely that the salt concentration was extremely low. This would give rise to a large effective diameter, and hence a large value of x. In fact, light scattering experiments seemed to indicate that the apparent or effective diameter was roughly ten times the physical diameter of the T.M.V. [1]. This would result in a value of $x = .64$ — much too large for the Onsager theory to be correct.

Oster [1] claimed excellent quantitative agreement with Onsager's theory. However, he used the approximate result given in Onsager's original paper, which was derived for the limiting case $x \ll 1$. He combined this result with the value of the second virial coefficient obtained from the light scattering experiments. In view of the previous discussion this seems somewhat absurd. The question which immediately springs to mind is how can such a procedure lead to good agreement with experimental results? However, since the parameters calculated from the Onsager theory for finite values of x are not greatly different from those for $x \rightarrow 0$ (see Appendix 1) Oster's calculation can be regarded as an extrapolation into the regime of large x. In other words, if the correct solution to the phase transition problem for large x is a smooth continuation of the Onsager result valid for small x, then Oster's procedure is reasonable. Of course this extrapolation cannot be carried too far, since as $x \rightarrow 1$, the transition is no longer isotropic-nematic but begins to resemble the "hard sphere" type transition.

The observed ratios of the concentrations of the two phases in

the coexistence region is 1.4, while the theoretical values range from 1.26 ($x \to 0$) to 1.11 ($x = .2$). These ratios appear to be too small, but this is probably the result of the neglect of the van der Waals forces. Attractive forces, however small, will tend to increase the coexistence region.

Bernal and Fankuchen [5] give results for the interparticle spacing of high density gels which are in equilibrium with the isotropic phase. Although the salt concentration is given, it is not clear how to interpret the results in the light of the Onsager theory. The hard rod model predicts only the transition concentrations, which are not unambiguously converted into interparticle spacings.

To conclude this section, it appears that the Onsager theory provides an explanation for the low density phase transitions observed in T.M.V. systems. At present experimental data is either lacking in crucial parameters or is outside the range of validity of the truncated virial expansion. A definitive test of the theory will require the *concentrations* of the coexisting phases as a function of the pH and ionic strength.

2.5 APPLICATION TO CLAYS

As with the T.M.V., van der Waals forces are weak at the spacing characteristic of the phase transition in clays [15]. The electrical double layer forces however are still significant at low salt concentrations. If the interaction is weak, the repulsive potential between parallel plates is given by [16]:

$$V = \frac{64nk_BT\gamma^2 e^{-\kappa R}}{\kappa} , \qquad (2.5.1)$$

where

$$\gamma = \frac{e^{e\psi_0/2k_BT} - 1}{e^{e\psi_0/2k_BT} + 1} .$$

Here n is the univalent salt concentrations, R is the interparticle spacing, ψ_0 is the surface potential, and $1/\kappa$ is the Debye screening length. Eqn (2.5.1) is valid for $\kappa R \gg 1$.

In order to utilize the results of Section 2.3, the clay sol can be modelled as a fluid of hard discs. The diameter of the discs is taken to be the average diameter of the clay particles, and the thickness is an effective thickness. As long as the electric field is large in a region smaller than the plate diameter ($\kappa d > 1$), then in a manner analogous with the T.M.V., the effective thickness is the distance at which the double layer energy is equal to $\alpha k_B T$. If $1/\kappa$ is not too large, the effective diameter is not a sensitive function of α. In the following calculations, $\alpha = 1/2$. From Eqn (2.5.1), this thickness l is given by

$$l = \frac{\log[32n\gamma^2\pi d^2/\kappa]}{\kappa} . \qquad (2.5.2)$$

For large values of the plate separation and a surface charge characteristic of clays (i.e. $e\psi_0/k_BT \ll 1$) it is easily shown that $\gamma^2 \sim 1$ [16]. In order to simplify the calculations, it has been assumed that the discs are parallel, but this obviously need not be the case. If the discs are at some angle to each other, then the double layer repulsion will be reduced. Thus Eqn (2.5.2) will tend to overestimate l. Some values of x are given in Table 2.2 for various values of the salt

Table 2.2

Electrolyte Concentration (M)	Effective Thickness (Å)		
	D = .1 μ	D = .5 μ	D = 1 μ
1.0	11	14	15
0.1	37	47	51
0.01	129	160	174
0.001	443	542	575

The effective thickness of a hard plate as a function of electrolyte concentration and plate diameter.

When $x \gtrsim .15$, the "apparent" volume fraction occupied by the clay is greater than 100% (Table 2.1). Eqn (2.3.2) is clearly inaccurate at large volume fractions, so that the results are valid only for $x < .15$.

If the surface area occupied by 1 gm of clay is taken to be 375×10^4 cm^2 [8], then the relation between ρd^3 and the concentration (by weight) is:

$$\rho d^3 = \frac{375 \, cd \, 10^4}{\pi/4}$$

$$= 477 \, cd \, 10^4 . \qquad (2.5.3)$$

Here c is the weight fraction of clay, and it is assumed that each plate is made up of one unit layer [8].

Langmuir observed that the dispersion became completely ordered at concentrations above 2.2%. Assuming that $d = 10^4$ Å, which is characteristic of clay plates, Eqn (2.5.3) gives $\rho_t d^3 = 10.5$. From Fig.

2.1, the lowest value of $\rho_t d^3$ (in the ordered phase) is 8.5 at x = .15.
Since Langmuir performed his experiments in very low salt solutions
(distilled water), it is probable that x will be larger than .15.
Consequently it is expected that $\rho_t d^3$ should be somewhat larger than 8.5.
However, in the regime of very low salt concentrations, three-body
interactions, which are ignored in Eqn (2.3.2), will become important.
The present theory will break down in this case; nevertheless it
appears that the trends are predicted correctly. From Fig. 2.1 it is
also clear that the ratio of the two phases appears to become constant
when x ≳ .05. At the limiting value of x = .15, the ratio is 1.12, in
good agreement with the observed value of 1.1.

It is evident from Fig. 2.1 that the transition concentration
increases as x increases. Recalling the relationship between salt
concentration and x, this gives rise to an interesting physical result.
If the ordered phase is in equilibrium with the disordered phase, the
addition of salt will cause the concentration in the ordered phase to
decrease, and *hence the particles will move further apart*. This is of
course contrary to what one would expect from DLVO theory.

The osmotic pressure is given as a function of dimensionless
density in Fig. 2.2. The coexistence region is clearly seen from the
characteristic flat portion of the curves. For clay plates of 1000 Å in
diameter, the pressure at the transition (x = .05) is $\sim 10^{-3}$ atm. This
pressure should be within the range of experimental observation.

Fig. 2.3 shows the distribution function $f(\theta)$ for the ordered
phase at the transition $(t/d = 0)$. The curves showing $f(\theta)$ for other
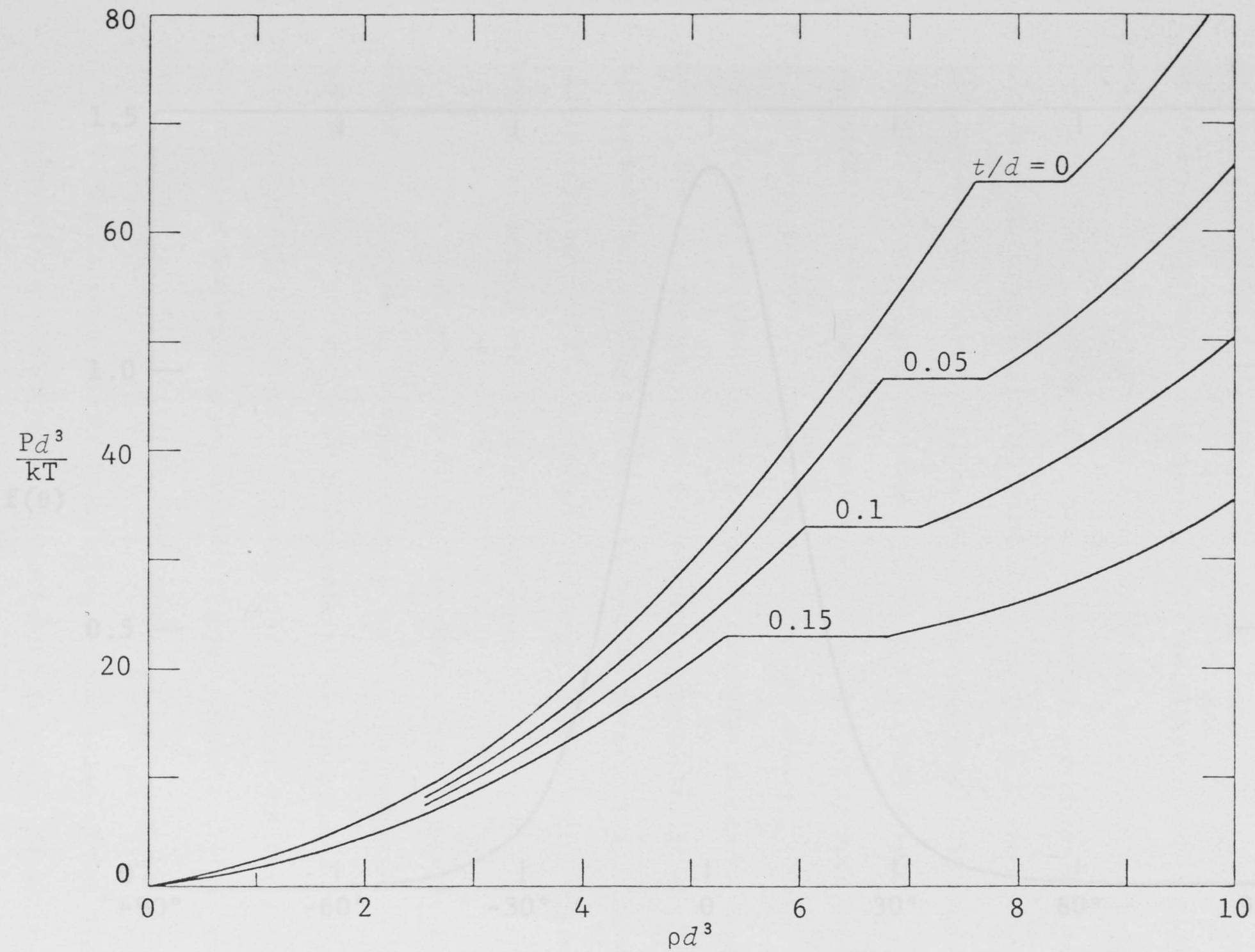values of t/d are very similar and hence are not shown.

Fig. 2.2: Dimensionless pressure of the hard plate fluid as a function of the density. The coexistence region can be clearly seen from the flat portions of the curves.
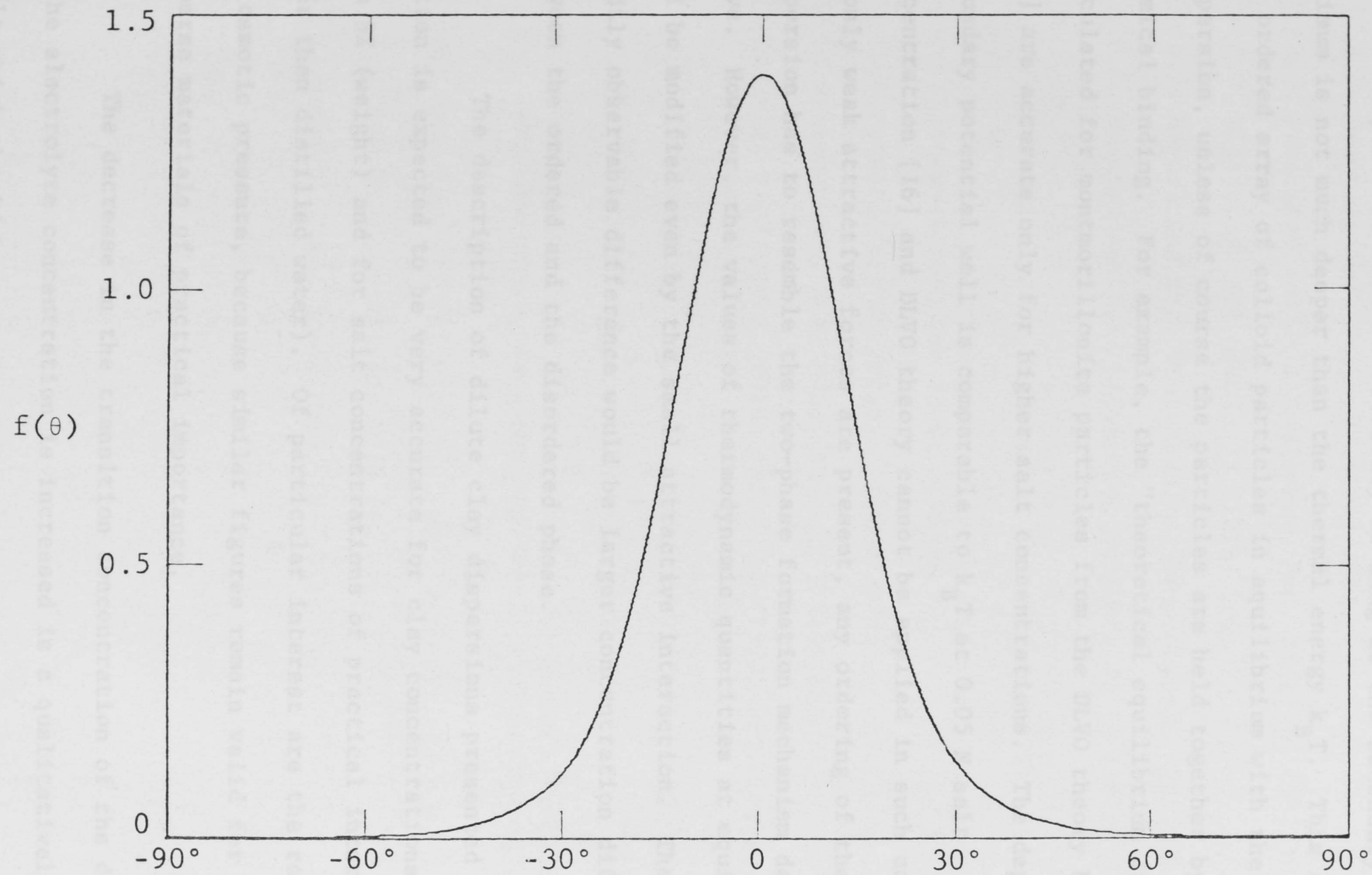
Fig. 2.3: The orientational distribution function $f(\theta)$ for the hard plate fluid at the transition ($x = 0$).

In this section we have only examined the behaviour of low density clay suspensions where attractive forces between the particles are negligible. However, the full statistical mechanics description of colloid dispersions will be necessary as long as the secondary potential minimum is not much deeper than the thermal energy k_BT. This applies to any ordered array of colloid particles in equilibrium with the dilute dispersion, unless of course the particles are held together by specific chemical binding. For example, the "theoretical equilibrium distances" calculated for montmorillonite particles from the DLVO theory by Norrish [16] are accurate only for higher salt concentrations. The depth of the secondary potential well is comparable to k_BT at 0.05 N salt concentration [16] and DLVO theory cannot be applied in such conditions. If only weak attractive forces are present, any ordering of the dispersion has to resemble the two-phase formation mechanism described above. However, the values of thermodynamic quantities at equilibrium will be modified even by the small attractive interaction. The most readily observable difference would be larger concentration difference between the ordered and the disordered phase.

The description of dilute clay dispersions presented in this section is expected to be very accurate for clay concentrations less than 5% (weight) and for salt concentrations of practical interest (e.g. other than distilled water). Of particular interest are the results for the osmotic pressure, because similar figures remain valid for poly-disperse materials of practical importance.

The decrease in the transition concentration of the dispersion as the electrolyte concentration is increased is a qualitatively new result which should be experimentally observable.

REFERENCES — CHAPTER 2

[1] G. Oster, *J. Gen. Physiol.* <u>33</u> (1949) 445.

[2] E.J. Rome, *J. Mol. Biol.* <u>27</u> (1967) 591.

[3] A.J. Coulombre and J.L. Coulombre, *Dev. Biol.* <u>28</u> (1972) 183.

[4] A.P. Minton, *J. Mol. Biol.* <u>75</u> (1973) 559.

[5] J.D. Bernal and I.J. Fankuchen, *J. Gen. Physiol.* <u>25</u> (1941) 111.

[6] S.L. Brenner and D.A. McQuarrie, *Biophys. J.* <u>13</u> (1973) 301, and the works cited therein.

[7] V.A. Parsegian and S.L. Brenner, *Nature* <u>259</u> (1976) 435.

[8] H. van Olphen, *An Introduction to Colloid Clay Chemistry* (Interscience, New York: 1963).

[9] I. Langmuir, *J. Chem. Phys.* <u>6</u> (1938) 873.

[10] L. Onsager, *Ann. N.Y. Acad. Sci.* <u>51</u> (1949) 627.

[11] See e.g. M.A. Carter, *Phys. Rev.* A <u>10</u> (1974) 625. This article gives a short review of previous work.

[12] J.P. Straley, *Mol. Cryst. Liqu. Cryst.* <u>22</u> (1973) 333.

[13] J.P. Straley, *Mol. Cryst. Liqu. Cryst.* <u>24</u> (1973) 7.

[14] M.R. Osborne and M.A. Sanders, in *Descent Methods in Optimization* (eds. Anderssen, Jennings and Ryan), (University of Queensland Press: 1972).

[15] P.A. Forsyth, jr., S. Marčelja, D.J. Mitchell and B.W. Ninham, *Proc. Int. Soc. Soil Sci. Conference* on 'Modification of Soil Structure', Adelaide, 1976 (in press).

[16] K. Norrish, *Disc. Farad. Soc.* <u>18</u> (1954) 120.

CHAPTER 3

SURFACE THERMODYNAMICS

3.1 SURFACE QUANTITIES

The subject of surface thermodynamics is undoubtedly confusing. This situation is not aided by the plethora of definitions of surface quantities. This chapter is not by any means an exhaustive review of the subject; it merely serves to give plausible arguments for the definitions which will be used in Chapter 4.

In the following the Gibbs convention for describing thermodynamic quantities of an interface will be used [1]. In this convention the interfacial region is considered to be a flat plane, called the Gibbs geometrical surface. (Only flat surfaces will be considered in this chapter.) Clearly the volume of this region, V^σ, is zero. The amount of the ith substance associated with the interface will be denoted by Γ_i, with dimensions of $(area)^{-1}$. The number of interfacial particles of the ith type is then $n_i = A\Gamma_i$, where A is the area of the surface. If the quantities of interest vary only in one direction, say the x direction, then the surface excess Γ_i is defined by:

$$\Gamma_i = \int_0^\infty \left(n_i(x) - n_i^+\right) dx + \int_{-\infty}^0 \left(n_i(x) - n_i^-\right) dx \ .$$

Here $n_i(x)$ is the actual number density of the ith species, and n_i^{+-} is

the bulk density as $x \to \pm\infty$.

The location of the interface (at $x = 0$) is for the moment arbitrary. However, it is usually possible to fix the origin of coordinates so that quantities which are of no interest, e.g. Γ_{H_2O}, are set equal to zero. In a manner analogous with bulk systems, it is possible to define surface potentials F^σ, G^σ, Ω^σ and so on.

Consider a region of finite volume V^σ containing the interface, which is characterized by a surface tension γ and an area A. The amount of material in this region may vary, but its volume and temperature are fixed. Since this region is in equilibrium with the bulk, the chemical potentials of all species μ_i are the same as in the bulk. The appropriate thermodynamic potential would appear to be some generalization of Ω, viz:

$$\Omega = -PV^\sigma + \gamma A$$

and letting $V^\sigma \to 0$ in accordance with the Gibbs convention:

$$\Omega^\sigma = \gamma A . \qquad (3.1.1)$$

In analogy with the bulk Ω [1]:

$$d\Omega^\sigma = -S^\sigma dT - \sum_i n_i^\sigma d\mu_i + \gamma dA , \qquad (3.1.2)$$

where γ is defined as:

$$\gamma = \left(\frac{\partial \Omega^\sigma}{\partial A} \right)_{\mu_i, T} , \qquad (3.1.3)$$

i.e. the work done to increase the area of the surface while maintaining equilibrium with the bulk. From now on, the superscript σ will be dropped, all quantities being surface quantities unless explicitly stated otherwise. The summation convention, implied summation over

repeated indices, will also be employed.

If $d(\mu_i n_i - \gamma A)$ is added to both sides of Eqn (3.1.2), the surface Gibbs free energy is obtained viz:

$$dG = -SdT - Ad\gamma + \mu_i\,dn_i$$

$$(3.1.4)$$

$$G = \mu_i n_i \;.$$

Adding $d(\gamma A)$ to both sides of Eqn (3.1.4) gives the surface Helmholtz free energy:

$$dF = -SdT + \mu_i\,dn_i + \gamma dA$$

$$(3.1.5)$$

$$F = \mu_i n_i + \gamma A \;.$$

All these equations are formally identical with the thermodynamic relations among bulk quantities. Note from Eqn (3.1.5) that $\gamma \neq F/A$ unless the dividing surface is defined so that the surface excess of all components is zero. This is usually only possible for pure substances, in which case $F = \Omega = \gamma A$.

The Gibbs-Duhem relation is immediately obtained from Eqn (3.1.4):

$$SdT + Ad\gamma + A\Gamma_i d\mu_i = 0 \;.$$

At constant temperature this implies:

$$d\gamma = -\Gamma_i\,d\mu_i \;. \qquad (3.1.6)$$

3.2 SURFACE TENSION IN SYSTEMS WITH ELECTRICAL DOUBLE LAYERS

Consider a system composed of dissociable surface active groups i, the dissociated ions j, and the non-surface active ions and inert electrolyte k. Thus Eqn (3.1.6) becomes:

$$d\gamma = -\Gamma_i d\mu_i - \Gamma_j d\mu_j - \Gamma_k d\mu_k . \qquad (3.2.1)$$

The electrochemical potential of the surface active ions may be split into two parts:

$$\mu_j = \mu_j' + q_j \psi , \qquad (3.2.2)$$

where q_j is the charge on the jth species, ψ is the surface potential, and μ_j' is the chemical part of the electrochemical potential. Substituting Eqn (3.2.2) into Eqn (3.2.1) gives:

$$d\gamma = -\Gamma_i d\mu_i - \Gamma_j d\mu_j' - q_j \Gamma_j d\psi - \Gamma_k d\mu_k . \qquad (3.2.3)$$

It is now assumed that:

$$\Gamma_j q_j = \sigma , \qquad (3.2.4)$$

where σ is the surface charge. This definition is rigorously true only if species j are insoluble. Otherwise Γ_j also includes the excess of j in the diffuse double layer, and the concept of a surface charge becomes more obscure. Eqn (3.2.4) becomes more or less true as long as the inert electrolyte concentration is large, so that the double layer is highly compressed [2].

The first two terms of Eqn (3.2.3) represent the non-electrical part of the surface tension, denoted by γ_0. Thus:

$$d(\gamma - \gamma_0) = -\sigma d\psi - \Gamma_k d\mu_k . \qquad (3.2.5)$$

Since this is an exact differential, it may be integrated in any convenient fashion, viz.:

$$-(\gamma - \gamma_0) \;=\; \left. \int_{\mu_1^0}^{\mu_1} \Gamma_1 d\mu_1 \right|_{\sigma=0,\mu_2^0,\mu_3^0,\ldots}$$

$$+ \ldots + \left. \int_{\mu_k^0}^{\mu_k} \Gamma_k d\mu_k \right|_{\sigma=0,\mu_1,\ldots,\mu_{k-1},\mu_{k+1}^0,\ldots}$$

$$+ \ldots + \left. \int_0^{\psi} \sigma d\psi \right|_{\mu_1,\mu_2,\mu_3,\ldots} \quad .$$

Here μ_k^0 is the chemical potential of the kth species in the reference state. If Γ_k are assumed zero when $\sigma = 0$, then:

$$\gamma - \gamma_0 \;=\; - \int_0^{\psi} \sigma d\psi \quad . \tag{3.2.7}$$

A similar derivation of the above result is given in refs. 2,3.

3.3 SURFACE ENERGIES

When deciding which of the thermodynamic potentials to use, it is important to bear in mind that each potential has a characteristic set of independent variables. Just as one does not use a cannon to shoot sparrows, it is better to tailor the choice of thermodynamic potentials to the task at hand.

Some colloidal particles, AgI for example, interact in such a way that the chemical potentials of all species remain constant. Consequently, the force between AgI particles is given by:

$$Y \;=\; \left(- \frac{\partial \Omega}{\partial y} \right)_{\mu_i, T, A} , \tag{3.3.1}$$

where Y is the force conjugate to the spatial variable y. If Eqn
(3.2.7) is substituted into Eqn (3.3.1), the result for flat plates a
distance y apart is:

$$\frac{Y}{A} = \frac{\partial}{\partial y} \int_0^{\psi_0} \sigma d\psi$$

which is the well known result [4].

However, in the case of monolayers or bilayers, some of the
surface active species may be characterized by a fixed number, say n_j,
and not a fixed chemical potential. (For example j may be an insoluble
lipid.) In this circumstance Ω is obviously not the appropriate
potential to use, and thus a change of variable seems indicated. If
$d(n_j \mu_j)$ is added to both sides of Eqn (3.1.2) the result is:

$$df = - SdT - n_i d\mu_i + \mu_j dn_j + \gamma dA$$

$$f = \Omega + n_j \mu_j .$$

(3.3.2)

This potential is unusual in that some of the μ's and some of the n's
are independent variables. In Chapter 4 this potential will be used in
discussing the possibility of an "electrostatic" phase separation.

REFERENCES — CHAPTER 3

[1] E.A. Guggenheim, *Thermodynamics: An Advanced Treatment for Chemists and Physicists* (North-Holland, Amsterdam: 1967).

[2] Th.A.J. Payens, *Phillips Res. Rep.* <u>10</u> (1955) 425.

[3] J.Th.G. Overbeek, in *Colloid Science* (ed. H.R. Kruyt), Vol. I, Chap. 4 (Elsevier, Amsterdam: 1952).

[4] E.J.W. Verwey and J.Th.G. Overbeek, *Theory of the Stability of Lyophobic Colloids* (Elsevier, Amsterdam: 1948).

CHAPTER 4

THE ELECTRICAL DOUBLE LAYER, FREE ENERGY
AND PHASE SEPARATIONS IN MONOLAYERS AND BILAYERS

4.1 INTRODUCTION

Phase separations and clustering of membrane components have been observed in a variety of mixed lipid bilayers and biological membranes [1-13]. In artificial lipid bilayers composed of zwitterionic lipids and/or cholesterol mixtures, these phase separations depend on temperature and composition. Both solid-liquid and liquid-liquid phases have been observed in studies on mixed zwitterionic lipid bilayers [2,5, 7,8]. When anionic lipids are present the phase separations also depend on such factors as $[Ca^{2+}]$ and pH [3,9,13].

The term "phase separation" used here is distinct from "phase transition" [8]. The former occurs in a multi-component membrane, when phases of different *composition* separate. The latter occurs in a one-component membrane. It is worth adding that asymmetric membranes may also be considered as having undergone a "vertical phase separation" of components as distinct from the "lateral phase separation" that will be discussed in the following.

4.2 THE THERMODYNAMIC POTENTIAL FOR
MONOLAYERS AND BILAYERS

Consider a planar membrane composed of a mixture of dissociable acidic lipids $AH \rightleftharpoons A^- + H^+$ and neutral lipids B (see Fig. 4.1). The "free energy" of the system is assumed to be dominated by the double layer energy (i.e. chain-chain interactions, specific head group interactions, etc., are assumed constant), and the molecular areas of AH, A^- and B are taken to be identical. Let:

$$\Gamma_A = \text{surface excess of } AH + A^- \text{ groups}$$

$$\Gamma_B = \text{surface excess of } \quad B \quad \text{groups}$$

$$\Gamma = \text{surface excess of } \quad A^- \quad \text{groups} \ .$$

If Γ_A and Γ_B are fixed, as in the case of some insoluble monolayers or bilayers, then the appropriate thermodynamic potential to use is f, given by (from Eqn (3.3.2)):

$$f = \gamma A + (\Gamma_A - \Gamma)\mu_{AH} + \Gamma_B \mu_B + \Gamma \mu_{A^-} + \Gamma \mu_{H^+} \ . \qquad (4.2.1)$$

The $\Gamma \mu_{H^+}$ term is included since the number of H^+ ions that dissociate (Γ) is determined by the surface active components.

Assuming that A^-, AH, B and H^+ are ideal, Eqn (4.2.1) becomes:

$$\frac{f}{A} = \gamma + (\Gamma_A - \Gamma)\left(\mu_{AH}^0 + k_B T \log(\Gamma_A - \Gamma)\right) + \Gamma_B\left(\mu_B^0 + k_B T \log \Gamma_B\right)$$

$$+ \Gamma\left(\mu_{A^-}^0 + k_B T \log \Gamma - e\psi_0\right) + \Gamma\left(\mu_{H^+}^0 + k_B T \log n_{H^+}\right) \ . \qquad (4.2.2)$$

Here ψ_0 is the surface potential, μ_i^0 is the chemical potential in the standard state, and n_{H^+} is the bulk hydrogen ion concentration, $[H^+]_\infty$. It is assumed that the H^+ ions that dissociate do not sensibly affect the bulk $[H^+]_\infty$.

A
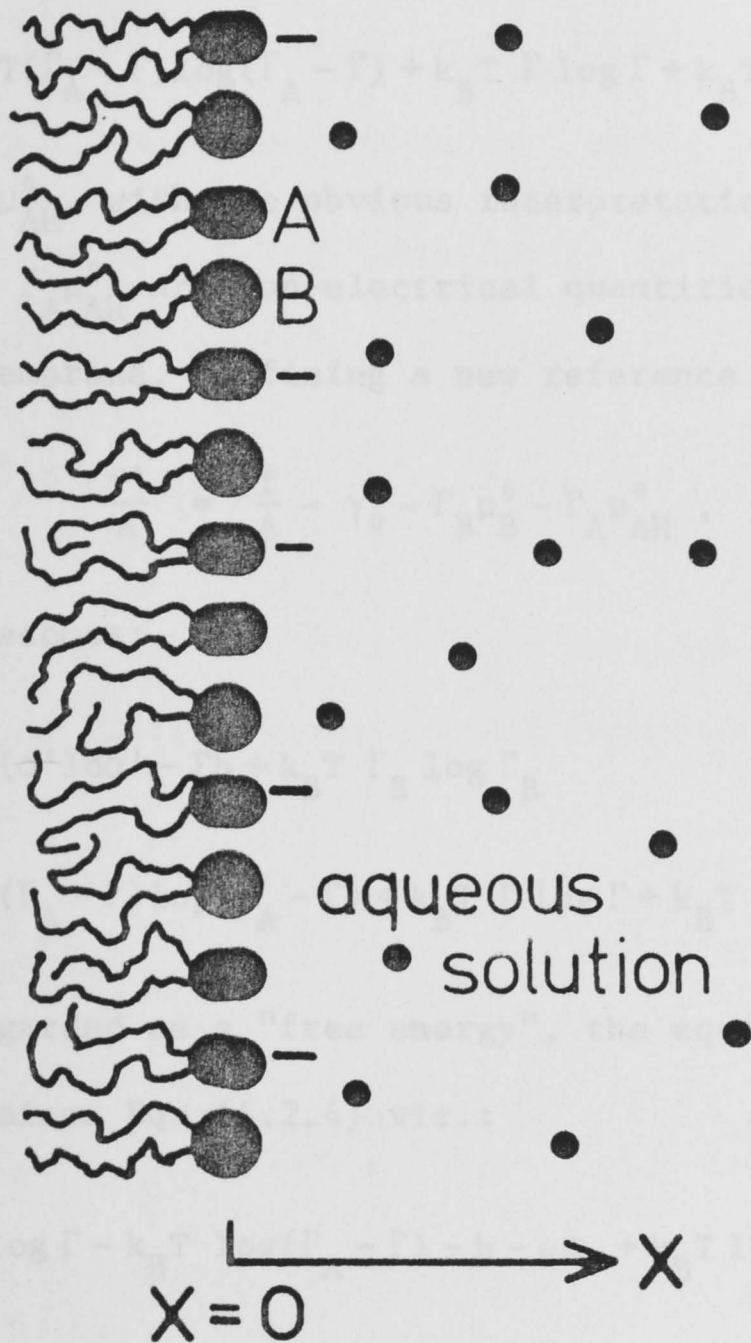B

aqueous
solution

X = 0

→ X

Fig. 4.1: Lipid-water interface. The lipids are a mixture of
dissociable lipids AH (e.g. phosphatidylserine) and undissociable
lipids B (e.g. cholesterol). The dissociable lipids are assumed to
be acidic, and these can be in the charged state A^- or uncharged
state AH.

Recalling that $\sigma = -\Gamma e$, Eqn (4.2.2) becomes:

$$\frac{f}{A} - \gamma_0 = \int_0^\sigma \psi(\sigma')d\sigma' + \Gamma_B \mu_B^0 + \Gamma_A \mu_{AH}^0 + \Gamma\left(\mu_{H^+}^0 + \mu_{A^-}^0 - \mu_{AH}^0\right) + k_B T \ \Gamma_B \log \Gamma_B$$

$$+ k_B T (\Gamma_A - \Gamma) \log(\Gamma_A - \Gamma) + k_B T \ \Gamma \log \Gamma + k_B T \ \Gamma \log n_{H^+} \ . \quad (4.2.3)$$

Let $-b = \mu_{H^+}^0 + \mu_{A^-}^0 - \mu_{AH}^0$, with the obvious interpretation of binding energy. The terms $\Gamma_B \mu_B^0$ and $\Gamma_A \mu_{AH}^0$ are non-electrical quantities, i.e. they refer to the uncharged membrane. Defining a new reference state by:

$$\frac{f'}{A} = \frac{f}{A} - \gamma_0 - \Gamma_B \mu_B^0 - \Gamma_A \mu_{AH}^0 \ ,$$

then Eqn (4.2.3) becomes:

$$\frac{f'}{A} = \int_0^\sigma \psi_0(\sigma')d\sigma' - \Gamma b + k_B T \ \Gamma_B \log \Gamma_B$$

$$+ k_B T (\Gamma_A - \Gamma) \log(\Gamma_A - \Gamma) + k_B T \ \Gamma \log \Gamma + k_B T \ \Gamma \log n_{H^+} \ . \quad (4.2.4)$$

Since f' may be regarded as a "free energy", the equilibrium value of Γ is that which minimizes Eqn (4.2.4) viz.:

$$\frac{\partial}{\partial \Gamma}\left(\frac{f'}{A}\right) = k_B T \log \Gamma - k_B T \log(\Gamma_A - \Gamma) - b - e\psi_0 + k_B T \log n_{H^+} = 0$$

or

$$\frac{\Gamma n_{H^+} \ e^{-e\psi_0/k_B T}}{\Gamma_A - \Gamma} = e^{b/k_B T}$$

$$= \text{constant} = K \ . \quad (4.2.5)$$

Since $\Gamma = [A^-]$, $n_{H^+} \ e^{-e\psi_0/k_B T} = [H^+]_{x=0}$ and $(\Gamma_A - \Gamma) = [AH]$, Eqn (4.2.5) is equivalent to

$$\frac{[A^-][H^+]_0}{[AH]} = K = \eta \ 10^{-pK} \ .$$

The constant K is readily identified as the reaction constant for the dissociation of the acidic lipid $AH \rightleftharpoons A^- + H^+$. K is related to the intrinsic or surface pK of the acidic lipid, which is of course not the same as the apparent pK (since $[H^+]_0 \neq [H^+]_\infty$) [14]. η is a constant of proportionality which depends on the units used.

Substituting Eqn (4.2.5) into Eqn (4.2.4), gives the equilibrium (minimum) free energy:

$$\frac{f'}{A} = e \int_0^{\psi_0} \Gamma(\psi_0') d\psi_0' + k_B T \; \Gamma_B \log \Gamma_B + k_B T \; \Gamma_A \log(\Gamma_A - \Gamma) \; . \quad (4.2.6)$$

Subtracting $(\Gamma_A + \Gamma_B) \log(\Gamma_A + \Gamma_B)$ (which is a constant for systems of fixed total number of lipids per unit area) from both sides of Eqn (4.2.6):

$$\frac{f'}{A} - (\Gamma_A + \Gamma_B) \log(\Gamma_A + \Gamma_B) = \frac{f^{el}}{A} = e \int_0^{\psi_0} \Gamma(\psi_0') d\psi_0' + k_B T \; \Gamma_B \; \log\left(\frac{\Gamma_B}{\Gamma_A + \Gamma_B}\right)$$

$$+ k_B T \; \Gamma_A \; \log\left(\frac{\Gamma_A}{\Gamma_A + \Gamma_B}\right) + k_B T \; \Gamma_A \; \log\left(\frac{\Gamma_A - \Gamma}{\Gamma_A}\right) \; . \quad (4.2.7)$$

A different derivation of this result in the limit $\Gamma_B \rightarrow 0$ has been given previously [15,16,17], but it is not as easily generalized as the above method.

4.3 GOUY-CHAPMAN THEORY

Consider the planar membrane of Fig. 4.1. The inert electrolyte solution is taken to be NaCl and $CaCl_2$. The number densities in the bulk ($x = \infty$) are:

$$n_+ = [Na + H^+]_\infty$$

$$n_{++} = [Ca^{2+}]_\infty$$

$$n_H = [H^+]_\infty = \eta \, 10^{-pH} \, ,$$

where η has the same meaning as before.

The one-dimensional Poisson equation is:

$$\frac{d^2\psi}{dx^2} = -4\pi \, \frac{\rho(x)}{\varepsilon} \, , \tag{4.3.1}$$

where $\rho(x)$ is the charge density as a function of x, ψ is the electro-static potential at x, and ε is the dielectric constant of water. The concentrations of the various ions in solution are given by the usual Boltzmann relation, viz.:

$$[Ca^{2+}]_x = n_{++} \, e^{-2e\psi/k_BT}$$

$$[Na^+ + H^+]_x = n_+ \, e^{-e\psi/k_BT} \tag{4.3.2}$$

$$[Cl^-]_x = [n_+ + 2n_{++}] \, e^{+e\psi/k_BT} \, .$$

Eqns (4.3.2) and (4.3.1) may be combined to give the Poisson-Boltzmann (P.B.) equation:

$$\frac{d^2\psi}{dx^2} = \frac{4\pi e}{\varepsilon} \left[(n_+ + 2n_{++}) \, e^{e\psi/k_BT} - 2n_{++} \, e^{-2e\psi/k_BT} - n_+ \, e^{-e\psi/k_BT} \right] . \tag{4.3.3}$$

Integrating this equation with the boundary condition $d\psi/dx \to 0$, $\psi \to 0$ as $x \to \infty$ yields:

$$\frac{1}{2}\left(\frac{d\psi}{dx}\right)^2 = \left(\frac{4\pi k_BT}{\varepsilon}\right) \left[(n_+ + 2n_{++}) \, e^{e\psi/k_BT} + n_{++} \, e^{-2e\psi/k_BT} \right.$$
$$\left. + n_+ \, e^{-e\psi/k_BT} - (2n_+ + 3n_{++}) \right] . \tag{4.3.4}$$

Since

$$\frac{d\psi}{dx}\bigg|_{x=0} = -\frac{4\pi\sigma}{\epsilon} = \frac{4\pi\Gamma e}{\epsilon}$$

then:

$$\Gamma = \left(\frac{\epsilon n_+ k_B T}{2\pi}\right)^{\frac{1}{2}} \frac{1}{e}\left(e^{-e\psi_0/k_B T} + (1+2c_1)\,e^{e\psi_0/k_B T}\right.$$

$$\left. + c_1\,e^{-2e\psi_0/k_B T} - (2+3c_1)\right)^{\frac{1}{2}} . \tag{4.3.5}$$

Here $c_1 = n_{++}/n_+$, and ψ_0 is the surface potential. The above development is standard (see e.g. ref. 18) except for the inclusion of $[H^+]_\infty$ in n_+. While this contribution is always negligible in comparison with the inert electrolyte concentrations, its inclusion is essential for a complete description of the double layer. This is because Γ and ψ_0 are related through Eqn (4.2.5).

4.4 LINEARIZED POISSON-BOLTZMANN EQUATION AND DISCRETE SURFACE CHARGE

If the full P.B. equation is linearized, the result is [19]:

$$\nabla^2 \psi - \kappa^2 \psi = 0 . \tag{4.4.1}$$

Here $1/\kappa$ is the Debye screening length [19]. The linearization procedure is valid for $|e\psi/k_B T| \ll 1$. If the average distance between charges a, is greater than $1/\kappa$, the discrete charge effects should become important. Consider a set of discrete charges on the x = 0 plane. The Eqn (4.4.1) becomes:

$$\nabla^2 \psi - \kappa^2 \psi = -\frac{4\pi q}{\epsilon} \sum_k \delta(x)\,\delta(\vec{\rho} - \vec{\rho}_k) . \tag{4.4.2}$$

Here $\vec{\rho}$ is a two-dimensional vector in the y-z plane and q is the charge

on the surface group. For the membrane in Fig. 4.1, the aqueous

solution is assumed to have a dielectric constant ε_1, and the membrane

itself ε_2. In most cases of interest $\varepsilon_2/\varepsilon_1 \ll 1$. Letting Φ represent

the two-dimensional Fourier transform of ψ, i.e.:

$$\Phi(x,\vec{q}) = \int d\vec{q}\ e^{i\vec{q}\cdot\vec{\rho}}\ \psi(x,\vec{\rho})$$

then Eqn (4.4.2) becomes:

$$\Phi_{zz} - (\kappa^2 + q^2)\Phi = -\frac{4\pi q}{\varepsilon}\sum_k e^{i\vec{\rho}_k\cdot\vec{q}}. \qquad (4.4.3)$$

The problem is now reduced to determining the Green's function, viz.:

$$G_{zz} - (\kappa^2 + q^2)G = \frac{\delta(x)}{\varepsilon}, \qquad (4.4.4)$$

where

$$\varepsilon = \varepsilon_1 \qquad x > 0$$
$$= \varepsilon_2 \qquad x < 0$$

$$\kappa^2 = \kappa^2 \qquad x > 0$$
$$= 0 \qquad x < 0.$$

The solution to Eqn (4.4.4) is:

$$G = -\frac{e^{-(\kappa^2+q^2)^{\frac{1}{2}}x}}{\varepsilon_1\left[(\kappa^2+q^2)^{\frac{1}{2}} + \frac{\varepsilon_2}{\varepsilon_1}q\right]} \qquad (x > 0)$$

$$\simeq -\frac{e^{-(\kappa^2+q^2)^{\frac{1}{2}}x}}{\varepsilon_1[\kappa^2+q^2]^{\frac{1}{2}}} \qquad \frac{\varepsilon_2}{\varepsilon_1} \ll 1.$$

Therefore

$$\Phi(x > 0) = \frac{4\pi q}{\varepsilon_1}\sum_k e^{i\vec{q}\cdot\vec{\rho}_k}\frac{e^{-(\kappa^2+q^2)^{\frac{1}{2}}x}}{(\kappa^2+q^2)^{\frac{1}{2}}},$$

$$\psi(x > 0) \; = \; \frac{4\pi q}{\varepsilon_1} \, \frac{1}{(2\pi)^3} \, \sum_k \int d\vec{q} \; e^{i\vec{q}\cdot(\vec{\rho}_k - \vec{\rho})} \; \frac{e^{-(\kappa^2 + q^2)^{\frac{1}{2}}x}}{(\kappa^2 + q^2)^{\frac{1}{2}}}$$

$$= \; \frac{2q}{\varepsilon_1} \sum_k \frac{e^{-\kappa|\vec{r} - \vec{\rho}_k|}}{|\vec{r} - \vec{\rho}_k|} \; . \tag{4.4.5}$$

In the linearized limit, with σ being a constant charge distribution:

$$\int d\vec{r} \int_0^{\psi_0} \sigma(\psi) d\psi \; = \; \tfrac{1}{2} \sigma \psi_0 A \; . \tag{4.4.6}$$

Since the charge distribution is no longer uniform, the discrete version of Eqn (4.4.6) is:

$$\int d\vec{r} \int_0^{\psi_0} \sigma(\psi) d\psi \; = \; \tfrac{1}{2} \int \rho(\vec{r}) \; \psi(\vec{r}) \; d\vec{r} \; .$$

Consequently the energy of the Nth surface charge will be:

$$\tfrac{1}{2} \int \rho_N(\vec{r}) \, \psi(\vec{r}) \, d\vec{r} \; = \; \tfrac{1}{2} \int q \; \delta(\vec{r} - \vec{\rho}_N) \sum_k \frac{2q}{\varepsilon_1} \frac{e^{-\kappa|\vec{r} - \vec{\rho}_k|}}{|\vec{r} - \vec{\rho}_k|} \, d\vec{r}$$

$$= \; \frac{q^2}{\varepsilon_1} \sum_k \frac{e^{-\kappa|\vec{\rho}_k - \vec{\rho}_N|}}{|\vec{\rho}_k - \vec{\rho}_N|} \; .$$

This sum contains an infinite term when $\vec{\rho}_k \to \vec{\rho}_N$. This represents the self-energy of a fundamental charge. In reality of course the self-energy of an electron is not infinite (i.e. an electron is not a point charge), but has some finite value. In any case the self-energy is merely a constant independent of the properties of the membrane, and can be neglected. Consequently the electrical energy of the Nth charge is:

$$\frac{\text{Energy}}{\text{Charge}} = \frac{q^2}{\varepsilon_1} \sum_{k, k \neq N} \frac{e^{-\kappa |\vec{\rho}_k - \vec{\rho}_N|}}{|\vec{\rho}_k - \vec{\rho}_N|} \ .$$

In order to simplify this result, the charge sites are assumed to be on a periodic array. This approximation is somewhat extreme, since the charge sites are much more randomly distributed in practice. However, making this assumption, the Energy/area is:

$$\frac{E^{el}}{A} = \frac{q^2}{\varepsilon_1 [\text{area of unit cell}]} \sum_{\substack{k \\ |\vec{\rho}_k| \neq 0}} \frac{e^{-\kappa |\vec{\rho}_k|}}{|\vec{\rho}_k|} \ .$$

The difference between this result and the free space result is a factor of ½. This is because of the discontinuity in ε at $x = 0$, and the assumption that $\varepsilon_2/\varepsilon_1 \ll 1$. If the lattice is square with repeat distance a, then:

$$\frac{E^{el}}{A} = \frac{q^2}{\varepsilon_1 a^3} \sum_{l,m}{}' \frac{e^{-\kappa a (l^2 + m^2)^{\frac{1}{2}}}}{(l^2 + m^2)^{\frac{1}{2}}} \ , \qquad (4.4.7)$$

where the prime indicates that the term with $l = m = 0$ is omitted.

4.5   FREE ENERGY

The free energy f^{el} for the monolayer is (Eqn (4.2.7)):

$$\frac{f^{el}}{A} = e \int_0^{\psi_0} \Gamma(\psi_0') d\psi_0' + \Gamma_B k_B T \log\left(\frac{\Gamma_B}{\Gamma_A + \Gamma_B}\right)$$

$$+ \Gamma_A k_B T \log\left(\frac{\Gamma_A}{\Gamma_A + \Gamma_B}\right) + \Gamma_A k_B T \log\left(\frac{\Gamma_A - \Gamma}{\Gamma_A}\right) \ . \qquad (4.5.1)$$

In the discrete case this becomes:

$$\frac{f^{el}}{A} = -\frac{q^2}{\epsilon_1} \Gamma^{\frac{3}{2}} \sum_{l,m}' \frac{e^{-\kappa \Gamma^{-\frac{1}{2}}(l^2+m^2)^{\frac{1}{2}}}}{(l^2+m^2)^{\frac{1}{2}}} + \Gamma_B k_B T \log\left(\frac{\Gamma_B}{\Gamma_A + \Gamma_B}\right)$$

$$+ \Gamma_A k_B T \log\left(\frac{\Gamma_A}{\Gamma_A + \Gamma_B}\right) + \Gamma_A k_B T \log\left(\frac{\Gamma_A - \Gamma}{\Gamma_A}\right) , \qquad (4.5.2)$$

where $\Gamma = 1/a^2$. Eqns (4.4.5) and (4.2.5) will determine ψ_0 and Γ for

fixed values of the other parameters. These results are substituted

into Eqn (4.5.2) to give the free energy.

On the other hand, the assumption of a continuous charge

distribution requires simultaneous solution of Eqns (4.2.5) and (4.3.5)

for Γ and ψ_0. These values are then substituted into Eqn (4.5.1). This

procedure requires some numerical computation and is described in

Appendix 2. The calculations were carried out for the continuous charge

distribution only; the many approximations involved in Eqn (4.5.2) make

this result somewhat doubtful.

4.6 PHASE SEPARATION

There have been several recent theoretical attempts to show

the effect of double layer energy changes on phase separations in

bilayer membranes. Some authors [9] have concluded that the double

layer energy favours a phase separation. However, these authors used γ

for the free energy, plus an entropy of mixing term. This is incorrect

for the reasons discussed in Chapter 3. More recently, another attempt

at this problem has been made [17]. This time the correct form of the

free energy (as $\Gamma_B \to 0$) was used, but charge dissociation was not taken

into account. Furthermore, these authors compared the free energy of

the states of "complete phase separation" and "homogeneous mixing". In other words, they compared the free energy difference between a bilayer membrane where charged lipids were scattered randomly throughout the membrane, and a bilayer where all the charged lipids clustered together. Since energy always favours a "mixed state", it was concluded that the double layer energy inhibits a phase separation. However, this procedure is incorrect in principle.

Consider the Gibbs free energy of a multi-component system, $G(T,\gamma,n_i)$. Let $X = n_1/(n_1+n_2)$, then the condition of thermodynamic stability is [20]:

$$\left(\frac{\partial^2 G}{\partial X^2}\right)_{n_2,n_3,\ldots,T,\gamma} > 0 .$$

In geometric terms, a graph of G vs. X must always be concave upwards. Regions where the curve is convex upwards are thermodynamically unstable. Systems which have such regions will phase separate; the values of X in each phase are determined by the double tangent construction [20].

In the case of the membrane described in the previous section, $X = \Gamma_A/(\Gamma_A+\Gamma_B)$. Recall that f can be derived from G by making two Legendre transformations, one on the pair γA, and the other on the pairs $n_j\mu_j$, where j is summed over the non-surface active species. Since X is determined from the ratio of surface active species, it follows from the properties of Legendre transformations that:

$$\left(\frac{\partial^2 G}{\partial X^2}\right)_{T,\gamma,n_2,n_3,\ldots} = \left(\frac{\partial^2 f}{\partial X^2}\right)_{\mu_1,T,A,n_2,n_3,\ldots,n_{i-1}} \qquad X = n_1/(n_1+n_2) ,$$

and therefore that f vs. X must also be concave upwards.

The free energy per particle $g = f^{el}/N$ was computed numerically

using Eqn (4.5.1). (Note that since

$$\frac{f'}{A} = \frac{f}{A} - \gamma_0 - \Gamma_B \mu_B^0 - \Gamma_A \mu_{AH}^0 \, ,$$

there should be linear terms in X added to g. However, these terms are of no importance as far as phase separations are concerned since they do not affect the second derivative. Alternatively, if $\mu_B^0 = \mu_{AH}^0$, then this additional term is independent of X.) The free energy/particle g was plotted as a function of X for a wide range of relevant parameters. Some of the results are shown in Figs. 4.2 and 4.3, for $T = 25$ °C, area per lipid = 60 $\overset{\circ}{A}^2$, and a dielectric constant for water of $\varepsilon = 80$. The inert electrolyte concentrations, [NaCl], [$CaCl_2$], and the (pH – pK) values are shown in the figures.

For low values of (pH – pK) there is little dissociation and hence the electrical energy contributes weakly to g. Consequently the ideal mixing term: $X \log X + (1-X) \log(1-X)$ dominates the expression for the free energy, and for (pH – pK) < 0 the curves are roughly symmetric about X = .5, with a minimum at X ∼ .5. For higher values of (pH – pK), the minimum shifts towards X = 1.

It was observed in all the curves generated that dg/dX was monotone increasing. This implies that this model does not exhibit a phase separation. Some of the curves were almost straight in the vicinity of X ∼ .5, particularly at higher pH and [Ca^{++}]. This suggests that only a small effect, due to some other interaction, is required to "nudge" the membrane into a phase separation. It is therefore necessary to examine what other factors could lead to a phase separation:

(1) First, the validity and applicability of the Poisson–Boltzmann equation must be justified. The P.B. equation has been found to work
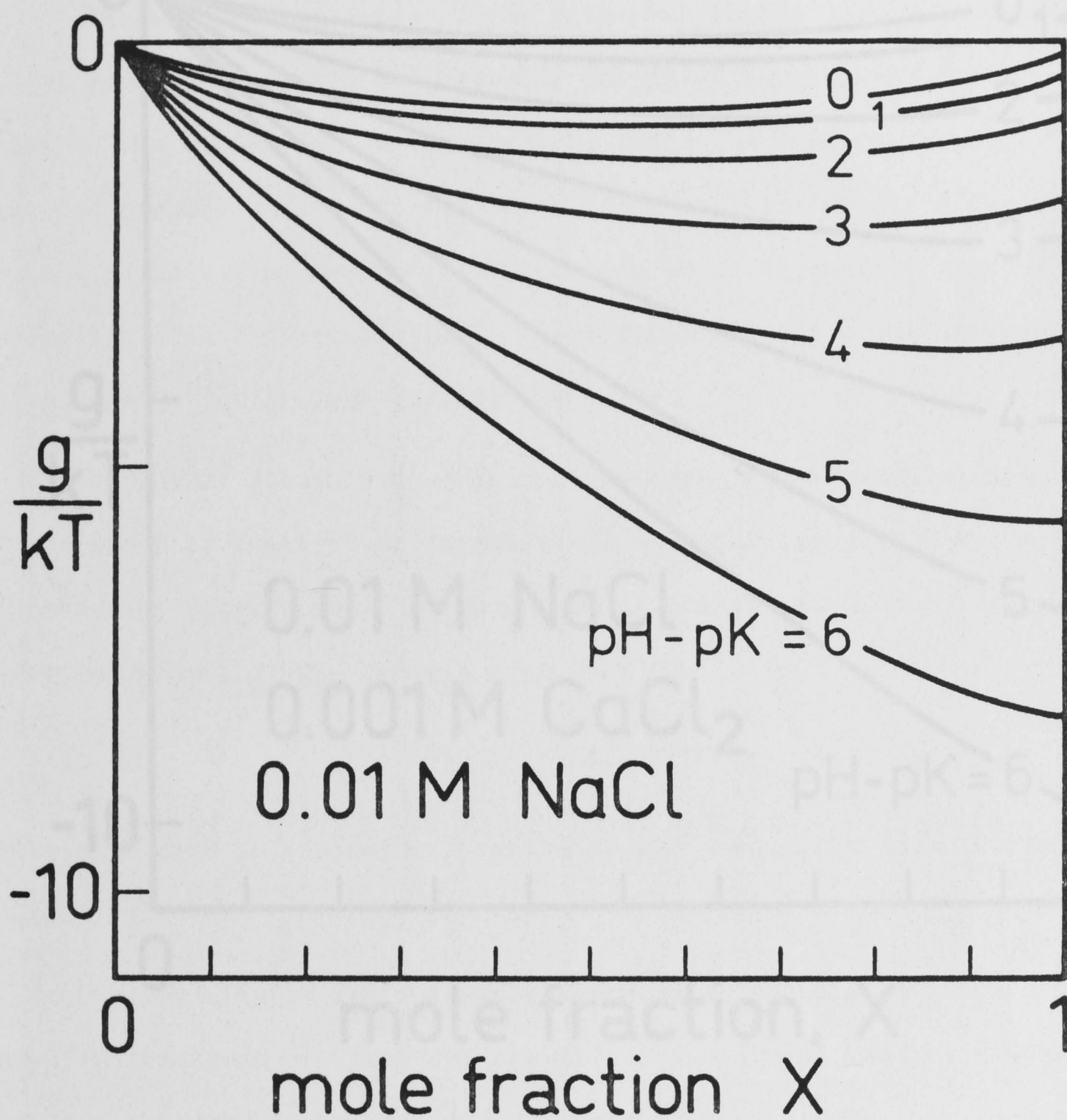
Fig. 4.2: Double layer molar free energy g as a function of mole
fraction $X = \Gamma_A/(\Gamma_A + \Gamma_B)$ for a two-component lipid layer consisting
of dissociable lipids AH (AH $\rightleftharpoons$ A$^-$ + H$^+$) and undissociable lipids B.
The curves are based on Eqn (4.5.1), and are plotted for a surface
area per head group of 60 $\overset{\circ}{A}^2$. The electrolyte is 0.01 M NaCl,
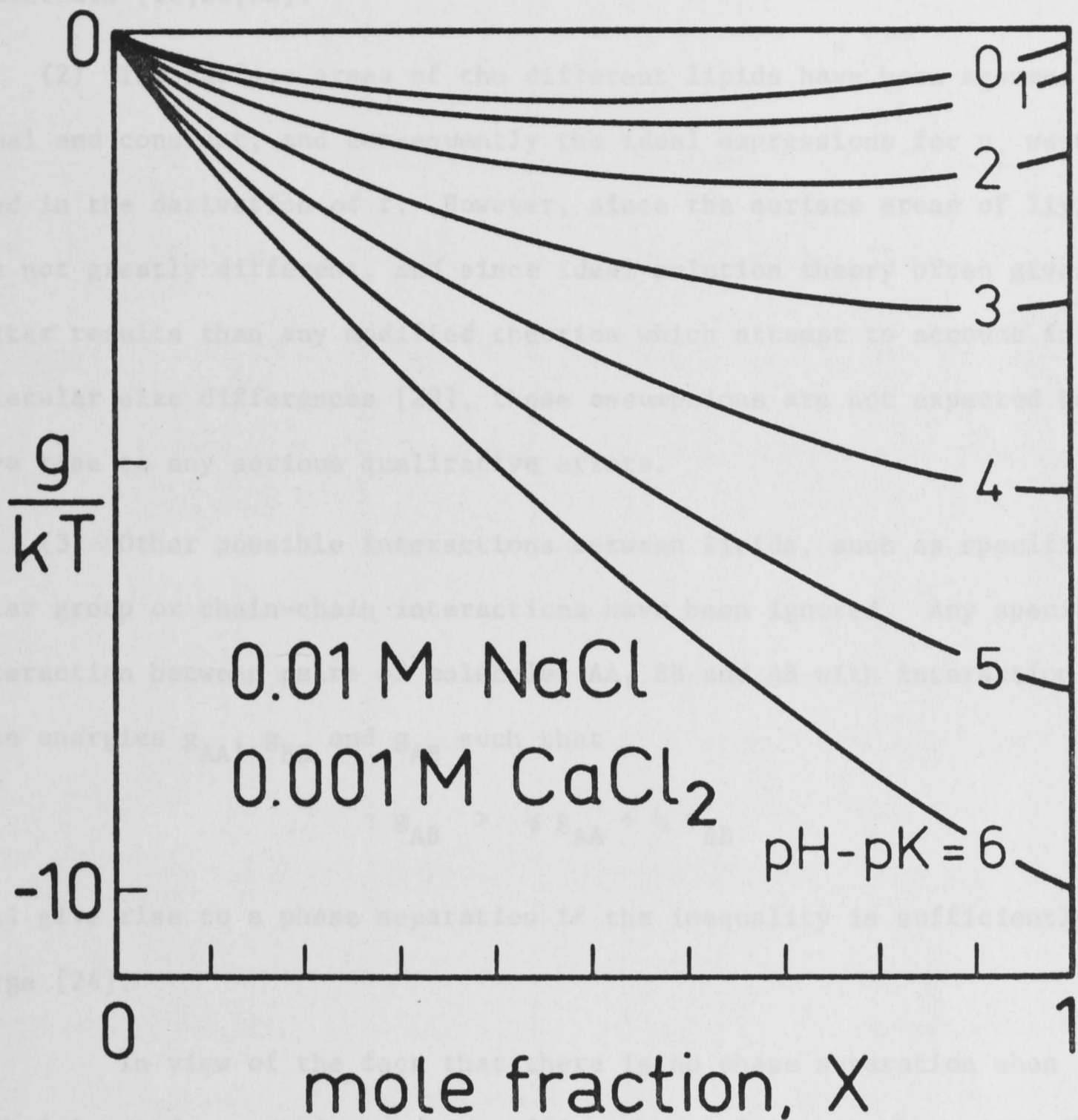T = 25 °C.

Fig. 4.3: Same as Fig. 4.2, but plotted for 0.01 M NaCl with 1 mM CaCl$_2$. Higher CaCl$_2$ concentrations do not modify the curves much more. Qualitatively similar results were obtained with 0.1 M NaCl. None of the curves obtained exhibited a phase separation. However, in all cases the curves become straighter (less curved) near X $\approx$ 0.5 as the pH and Ca^{2+} concentration increases. This indicates that phase separations, arising from some other type of interaction, would be more favourable at higher pH and [Ca^{2+}], as often observed.

surprisingly well in a variety of membrane studies, even at high surface potentials [18,21,22].

(2) The surface areas of the different lipids have been assumed equal and constant, and consequently the ideal expressions for μ_i were used in the derivation of f. However, since the surface areas of lipids are not greatly different, and since ideal solution theory often gives better results than any modified theories which attempt to account for molecular size differences [23], these assumptions are not expected to give rise to any serious qualitative errors.

(3) Other possible interactions between lipids, such as specific polar group or chain-chain interactions have been ignored. Any specific interaction between pairs of molecules AA, BB and AB with interaction free energies g_{AA}, g_{BB} and g_{AB} such that

$$g_{AB} > \tfrac{1}{2} g_{AA} + \tfrac{1}{2} G_{BB}$$

will give rise to a phase separation if the inequality is sufficiently large [24].

In view of the fact that there is no phase separation when such interactions are ignored, specific interactions must be responsible for the observed phase separation in membranes. However, in view of the "straightness" of some of the curves in Figs. 4.2 and 4.3, this specific interaction need not be very large.

REFERENCES — CHAPTER 4

[1] M.C. Philips and H. Hauser, *Chem. Phys. Lipids* 8 (1972) 127.

[2] E.J. Shimshick and H.M. McConnell, *Biochem. Biophys. Res. Comm.* 51 (1973) 446.

[3] S. Ohuishi and I. Tadunao, *Biochem. Biophys. Res. Comm.* 51 (1973) 132.

[4] C.D. Linden, K.L. Wright, H.M. McConnell and C.F. Fox, *Proc. Natl. Acad. Sci. USA* 70 (1973) 2271.

[5] C.W.M. Grant, S.H.W. Wu and H.M. McConnell, *Biochim. Biophys. Acta* 363 (1974) 151.

[6] S.W. Hui and D.F. Parsons, *Science* 190 (1975) 383.

[7] S.H.W. Wu and H.M. McConnell, *Biochemistry* 14 (1975) 847.

[8] E.J. Shimshick and H.M. McConnell, *Biochemistry* 12 (1973) 2351.

[9] H.J. Galla and E. Sackmann, *Biochim. Biophys. Acta* 401 (1975) 509.

[10] C.W.M. Grant, *Biophys. J.* 15 (1975) 949.

[11] W. Kleeman and H.M. McConnell, *Biochim. Biophys. Acta* 419 (1976) 206.

[12] C.R. Hackenbrock and K.J. Miller, *J. Cell. Biol.* 65 (1975) 615.

[13] D. Papahadjopoulos and G. Poste, *Biophys. J.* 15 (1975) 945.

[14] R.C. McDonald, S.A. Simon and E. Baer, *Biochemistry* 15 (1976) 885.

[15] Th.A.J. Payens, *Phillips Res. Rep.* 10 (1955) 425.

[16] F. Jahnig, *Biophys. Chem.* 4 (1976) 306.

[17] H. Trauble, M. Teubner, P. Woolley and H. Eibl, *Biophys. Chem.* 4 (1976) 319.

[18] R.V. Muller and A. Finkelstein, *J. Gen. Physiol.* 60 (1972) 285.

[19] E.J.W. Verwey and J.Th.G. Overbeek, *Theory of the Stability of Lyophobic Colloids* (Elsevier, Amsterdam: 1948).

[20] A.H. Wilson, *Thermodynamics and Statistical Mechanics* (Cambridge University Press: 1957).

[21]   S.G.A. McLaughlin, G. Szabo and G. Eisenman, *J. Gen. Physiol.* 58
       (1971) 667.

[22]   R.V. Muller and A. Finkelstein, *Proc. Natl. Acad. Sci. USA* 71
       (1974) 923.

[23]   R.A. Robinson and A.H. Stokes, *Electrolyte Solutions* (Butterworths,
       London: 1959), Chap. 9.

[24]   H.J. Hermans, in *Colloid Science* (ed. H.R. Kruyt), Vol. II
       (Elsevier, Amsterdam: 1949), pp.49-92.

CHAPTER 5

THE ORDERING OF WATER NEAR AN INTERFACE

5.1 INTRODUCTION

For some time it has been known that the properties of water near an interface are different from the properties of bulk water [1]. The commonly accepted view is that this interfacial water is frozen or ice-like; this appears to provide a qualitative explanation for some of the phenomena in solvation chemistry [2]. Experiments on lecithin bilayers have indicated that water near the lecithin-water boundary is highly structured [3]. Recent measurements [4] have also shown that there is a strong force between lecithin bilayers, apparently due to this frozen water.

The behaviour of aqueous non-electrolytes seems to indicate that there is a strong attractive solute-solute interaction of unknown origin [5]. In the case of hydrophobic solutes, this interaction is known as the hydrophobic interaction.

A recent theory [6], which was originally developed to explain the repulsive force between lecithin bilayers, has apparently yielded a qualitative explanation of these phenomena. A brief summary of the theory to date will be given here.

Because of the strong tetrahedral co-ordination of water,

resulting from hydrogen bonding, any disturbance in the water structure will cause a non-local response. In other words the perturbation induced by a boundary will be felt some distance away from this boundary. (Note that this is primarily an *angular* correlation, resulting from the tetrahedral co-ordination of water, and hence is not reflected in the angle averaged radial distribution function.)

In the neighbourhood of a perturbation, the properties of the water are assumed to decay continuously to the bulk values. This will occur when the distance from the perturbation exceeds some characteristic length, known as the correlation length. The commonly held view is that solute hydration is confined to the first shell of bound water molecules [7]. The concept of a continuous fall-off in the response to a disturbance is a new facet of this theory. It is this non-local response to a perturbation which leads to interactions between surfaces.

The ordering of water near an interface can be described by a scalar order parameter, $\eta(\vec{r})$, which varies continuously from point to point. This parameter can be imagined to represent the degree of tetra-hedral co-ordination of a water molecule. In terms of a Pople [8] theory of water, $\eta(\vec{r})$ could represent the "stiffness" of hydrogen bonds. The definition is deliberately left obscure — specific models of water lead to different interpretations of $\eta(\vec{r})$.

The deviation from bulk order $\varepsilon(\vec{r})$ is defined as:

$$\varepsilon(\vec{r}) = \eta(\vec{r}) - \eta_{bulk} .$$

Assuming that $\varepsilon(\vec{r})$ is small, then the free energy density may be expressed as an expansion in terms of $\varepsilon(\vec{r})$ and its derivatives. If it

is assumed that any non-zero $\varepsilon(\vec{r})$ or spatial change in $\varepsilon(\vec{r})$ will

increase the free energy, then the expansion of the free energy density

$f(\vec{r})$ is:

$$f(\vec{r}) = b\,\varepsilon(\vec{r})^2 + c[\vec{\nabla}\varepsilon(\vec{r})]^2 + \ldots , \qquad (5.1.1)$$

where higher order terms have been ignored. The form of Eqn (5.1.1) is

quite general, as long as $\vec{\varepsilon}(r)$, $\vec{\nabla}\varepsilon(\vec{r})$ are small. This is of course why

the definition of $\eta(\vec{r})$ was left imprecise. As will be seen, it is

possible to draw some quite general conclusions *without specifying a*

particular model of water which defines $\eta(\vec{r})$ *precisely*.

To a first approximation then, the total free energy F is:

$$F = \frac{b}{\kappa^2} \int_V [(\vec{\nabla}\varepsilon)^2 + \kappa^2\varepsilon^2]\,d\vec{r} ; \qquad (5.1.2)$$

here $1/\kappa = (c/b)^{\frac{1}{2}}$. The functional form of $\varepsilon(\vec{r})$ is determined by

minimization of Eqn (5.1.2), with the result that:

$$[\nabla^2 - \kappa^2]\,\varepsilon(\vec{r}) = 0 . \qquad (5.1.3)$$

Since this is a continuous theory, it is possible to conceive

of a "point disturbance". The response of the water to this type of

perturbation will take the form of the Green's function of Eqn (5.1.3),

viz.:

$$G(\vec{r},\vec{r}') = \frac{e^{-\kappa|\vec{r} - \vec{r}'|}}{|\vec{r} - \vec{r}'|} .$$

Thus the order is "propagated" by the function $G(\vec{r},\vec{r}')$ with a decay

length of $1/\kappa$. This length $1/\kappa$, can be identified as the order

parameter correlation length. From the form of $G(\vec{r},\vec{r}')$ it is clear that

the expansion of Eqn (5.1.1) is equivalent to assuming the Ornstein-

Zernike form for the correlation of the order parameter.

Eqn (5.1.1) has the same form as the Landau expansions [9] familiar from the study of phase transitions. Although these expansions were originally devised for properties near the critical point, it is clear that Eqn (5.1.1) remains valid as long as $\varepsilon(\vec{r})$ and the spatial rate of change of $\varepsilon(\vec{r})$ are small. A similar type of expansion was also used by Cahn and Hilliard [10] in their studies of interfacial energies.

The coefficients b and c can be derived *a priori* from specialized models of water. It is possible to use a generalized version of the Pople model of water to derive the form of Eqn (5.1.1) and the values of the coefficients [11]. However, rather than become involved in a debate about the merits of different models of water, the coefficients b and c will be regarded as phenomenological parameters, to be obtained, where possible, by comparison with experimental results.

Eqn (5.1.2) may be transformed into a surface integral, viz.:

$$F \;=\; \frac{b}{\kappa^2} \int_S \vec{\varepsilon}(r) \; \vec{\nabla}\varepsilon(r) \; d\vec{s} \;, \qquad (5.1.4)$$

where s is the perturbing boundary in the solvent. If the boundary condition for Eqn (5.1.3) is $\varepsilon(\vec{r}) = \varepsilon_0$ on s, then Eqn (5.1.4) can be rewritten as:

$$F \;=\; \frac{b\varepsilon_0^2}{\kappa^2} \int_S \psi\vec{\nabla}\psi \; d\vec{s} \;, \qquad (5.1.5)$$

where ψ is the solution of $[\nabla^2 - \kappa^2]\psi = 0$ with $\psi = 1$ on s, and $d\vec{s}$ is along the *outer* normal to v.

Consider an aqueous non-electrolyte solution. If two solute molecules are a distance d apart, then:

$$F_{12} = F(d) - F(\infty) \qquad (5.1.6)$$

gives the contribution to the potential of mean force between the solute

molecules arising from the change in solvent structure. If the solute

molecules are considered to be hard spheres, then F_{12} is determined by

the solution of Eqn (5.1.3) subject to the boundary condition $\varepsilon(\vec{r}) = \varepsilon_0$

on the surface of the two spheres. This procedure is described in the

following section. Readers who are uninterested in the manipulation of

modified spherical Bessel functions of the first and second kinds are

well advised to skip to Section 5.3!

5.2 DETERMINATION OF THE SOLUTE-SOLUTE POTENTIAL

Consider two identical spheres each of radius R. The centres

of the two spheres are at $\vec{r}_1$ and $\vec{r}_2$, with azimuthal angles θ_1 and θ_2

respectively. These angles are referred to the axis $\vec{r}_1 - \vec{r}_2$. The

equation to be solved is:

$$[\nabla^2 - \kappa^2]\psi = 0 . \qquad (5.2.1)$$

The solution of Eqn (5.2.1) can be expressed as:

$$\psi(\vec{r}) = \sum_{M=0}^{\infty} a_M K_M(\kappa|\vec{r} - \vec{r}_2|) \, P_M(\cos\theta_2)$$

$$+ \sum_{N=0}^{\infty} a_N K_N(\kappa|\vec{r} - \vec{r}_1|) \, P_N(\cos\theta_1) . \qquad (5.2.2)$$

Here $K_N(z)$ are the modified spherical Bessel functions of the second

kind [12], and $P_N(x)$ are the Legendre polynomials. The unknown a_N are

determined by applying the boundary condition $\psi = 1$ on s_1, s_2. This is

most easily done if $K_M(\kappa|\vec{r} - \vec{r}_2|) \, P_M(\cos\theta_2)$ is expressed as a linear

combination of $K_l(\kappa|\vec{r} - \vec{r}_1|)\ P_l(\cos\theta_1)$, and the boundary condition imposed on s_1.

An addition theorem for spherical Hankel functions has been derived in ref. [13]. The formula simplifies somewhat for the case of azimuthal symmetry, viz.:

$$H_M^1(\kappa|\vec{r} - \vec{r}_2|)\ P_M(\cos\theta_2)$$

$$= \sum_{N=0}^{\infty}\ (2N+1)\ U_{MN}(\kappa|\vec{r}_1 - \vec{r}_2|)\ J_N(\kappa|\vec{r} - \vec{r}_1|)\ P_N(\cos\theta_1)\ , \quad (5.2.3)$$

where

$$U_{MN}(z)\ =\ \sum_{r=0}^{M}\ (-1)^r\ \frac{\Gamma(M - r + \tfrac{1}{2})\ \Gamma(N - r + \tfrac{1}{2})\ \Gamma(r + \tfrac{1}{2})}{\Gamma(M + N - r + \tfrac{3}{2})\ \Gamma(\tfrac{1}{2})^2}$$

$$\times\ \frac{(M + N - r)!\ (M + N - 2r + \tfrac{1}{2})!}{(M - r)!\ (N - r)!\ r!}\ H_{M+N-2r}^1(z)\ . \quad (5.2.4)$$

Here $H_M^1(z)$ is the spherical Hankel function of the first kind, and $J_l(z)$ is the spherical Bessel function of the first kind [12]. The following relations will prove useful [12]:

$$H_l^1\left(z\ e^{i\pi/2}\right)\ =\ K_l(z)\ \frac{2}{\pi}\ e^{-ie\pi/2}$$

$$J_l\left(z\ e^{i\pi/2}\right)\ =\ I_l(z)\ e^{ie\pi/2}$$
$$\qquad\qquad -\pi \leqslant \arg z \leqslant \frac{\pi}{2}\ , \quad (5.2.5)$$

where $K_l(z)$ has the same meaning as before, and $I_l(z)$ is the modified spherical Bessel function of the first kind [12]. If $\kappa \to e^{i\pi/2}\kappa$ in Eqn (5.2.4), then with the aid of Eqn (5.2.5), the addition theorem becomes:

$$K_M(\kappa|\vec{r} - \vec{r}_2|)\ P_M(\cos\theta_2)$$

$$= \sum_{N=0}^{\infty}\ (2N+1)\ B_{MN}\ I_N(\kappa|\vec{r} - \vec{r}_1|)\ P_N(\cos\theta_1)\ , \quad (5.2.6)$$

where

$$B_{MN} = \sum_{r=0}^{M} A_{MN}^r (-1)^r K_{M+N-2r}(\kappa|\vec{r}_1 - \vec{r}_2|)$$

$$A_{MN}^r = (-1)^r \frac{\Gamma(M-r+\frac{1}{2}) \; \Gamma(N-r+\frac{1}{2}) \; \Gamma(r+\frac{1}{2})}{\Gamma(M+N-r+\frac{3}{2}) \; [\Gamma(\frac{1}{2})]^2}$$

$$\times \frac{(M+N-r)! \; (M+N-2r+\frac{1}{2})!}{(M-r)! \; (N-r)! \; r!} \; .$$

Substituting Eqn (5.2.6) into Eqn (5.2.2) gives:

$$\psi(\vec{r}) = \sum_{N=0}^{\infty} a_N K_N(\kappa|\vec{r} - \vec{r}_2|) \; P_N(\cos\theta_1)$$

$$+ \sum_{M=0}^{\infty} a_M \sum_{N=0}^{\infty} (2N+1) \; B_{MN} \; I_N(\kappa|\vec{r} - \vec{r}_1|) \; P_N(\cos\theta_1) \; . \quad (5.2.7)$$

Taking the inner product of both sides of Eqn (5.2.7) with respect to $P_j(\cos\theta_1)$, and evaluating the result on $s_1 (|\vec{r} - \vec{r}_1| = R)$ gives:

$$[\psi_s, P_j(\cos\theta_1)] = ||P_j(\cos\theta)||^2 \; a_j K_j(\kappa R)$$

$$+ \sum_{M=0}^{\infty} a_M (2j+1) \; B_{Mj} I_j(\kappa R) ||P_j(\cos\theta)||^2. \quad (5.2.8)$$

If $\psi_s = 1$ on s_1, then Eqn (5.2.8) becomes:

$$\delta_{j0} = a_j K_j(\kappa R) + \sum_{M=0}^{\infty} a_M (2j+1) \; B_{Mj} I_j(\kappa R) \; . \quad (5.2.9)$$

Let:

$$A_j = a_j K_j(\kappa R) \quad (5.2.10)$$

then Eqn (5.2.9) becomes:

$$\delta_{j0} = \sum_{M=0}^{\infty} \delta_{jM} A_M + \sum_{M=0}^{\infty} (2j+1) \; B_{Mj} \frac{I_j(\kappa R) \; A_M}{K_M(\kappa R)} \; . \quad (5.2.11)$$

Defining:

$$L_{jM} = (2j+1) B_{Mj} \frac{I_j(\kappa R)}{K_M(\kappa R)} \tag{5.2.12}$$

then Eqn (5.2.11) becomes:

$$\delta_{j0} = \sum_{M=0}^{\infty} \delta_{jM} A_M + \sum_{M=0}^{\infty} L_{jM} A_M \tag{5.2.13}$$

or in matrix form:

$$[\underset{\sim}{L} + \underset{\sim}{1}] \cdot \vec{A} = \vec{e}_1 , \tag{5.2.14}$$

where

$$[\vec{e}_1]_i = \delta_{i0}$$

$$[\underset{\sim}{1}]_{ij} = \delta_{ij} .$$

Consequently, once the elements of the matrix $\underset{\sim}{L}$ are calculated for given κR and κd $(d = |\vec{r}_1 - \vec{r}_2|)$, then the A_i (and hence the a_i) are determined from the infinite set of linear equations [Eqn (5.2.14)]. For numerical purposes of course, $\underset{\sim}{L}$ must be truncated. If the matrix elements $L_{jM} \to 0$ sufficiently rapidly as $j,M \to \infty$, this procedure should converge. It is easy to show from the asymptotic form of Bessel functions for order >> argument that [12]:

$$L_{jM} \sim \frac{[2(M+j)-1]!!}{(2M-1)!! \, (2j-1)!!} \left(\frac{\kappa R}{\kappa d}\right)^{M+j} , \tag{5.2.15}$$

where

$$\rho!! = \rho(\rho-2)(\rho-4) \ldots .$$

It is obvious by inspection of Eqn (5.2.15) that

$$\underset{j \to \infty}{Lim} L_{jM} = 0 \qquad M \text{ fixed}$$

$$\underset{M \to \infty}{Lim} L_{jM} = 0 \qquad j \text{ fixed}$$

as long as $(\kappa R/\kappa d) < 1$. In other words, along any row or column, $L_{jM} \rightarrow 0$, as long as the centre-to-centre distance is less than the radius of a sphere. On the diagonal, Eqn (5.2.15) becomes, for $j, M \gg 1$:

$$L_{jj} \sim \frac{[4j]!!}{(2j)!! \,(2j)!!} \left(\frac{\kappa R}{\kappa d}\right)^{2j}, \qquad (5.2.16)$$

Taking logarithms of both sides of Eqn (5.2.16) and using Stirling's approximation yields:

$$\underset{j \rightarrow \infty}{L_{jj}} \sim \left(\frac{2\kappa R}{\kappa d}\right)^{2j}.$$

This goes to zero as $j \rightarrow \infty$ when $(\kappa R/\kappa d) < \frac{1}{2}$. This result is physically reasonable, i.e. the scheme for determining the a_i should converge as long as the two spheres are not touching.

The energy of interaction between the two spheres is [Eqn (5.1.5)]:

$$F(d) = \frac{b\varepsilon_0^2}{\kappa^2} \int_{s_1 + s_2} \psi \vec{\nabla} \psi \cdot d\vec{s}$$

$$= -\frac{2b\varepsilon_0^2}{\kappa^2} \int_{s_1} \psi \frac{\partial \psi}{\partial n} \, ds. \qquad (5.2.17)$$

Substituting Eqn (5.2.7) into Eqn (5.2.17) and performing the indicated integration gives:

$$F(\kappa d) = -2b\varepsilon_0^2 \frac{4\pi R^2}{\kappa} \left(-A_0 \frac{K_1(\kappa R)}{K_0(\kappa R)} + \sum_{M=0}^{\infty} \frac{A_M B_{MO} I_1(\kappa R)}{K_M(\kappa R)}\right). \qquad (5.2.18)$$

Since $B_{MO} \rightarrow 0$ as $\kappa d \rightarrow \infty$, and $A_0 \rightarrow 1$ as $\kappa d \rightarrow \infty$:

$$F(\infty) = 2b\varepsilon_0^2 \frac{4\pi R^2}{\kappa} [1 + 1/(\kappa R)] \qquad (5.2.19)$$

which is of course just twice the single sphere energy. Combining Eqn

(5.2.18) and Eqn (5.2.19) gives:

$$F_{12}(d) = \frac{2b\varepsilon_0^2}{\kappa} 4\pi R^2 \left[A_0 \frac{K_1(\kappa R)}{K_0(\kappa R)} - \sum_{M=0}^{\infty} \frac{A_M B_{MO} I_1(\kappa R)}{K_M(\kappa R)} - (1 + 1/[\kappa R]) \right] .$$ (5.2.20)

This is the final result. The matrix Eqn (5.2.14) can be inverted by

expanding $[\underset{\sim}{L} + \underset{\sim}{1}]^{-1}$, viz.:

$$\vec{A} = [\underset{\sim}{1} - \underset{\sim}{L} + \underset{\sim}{L}^2 + \ldots] \cdot \vec{e}_1$$

since L_{ij} are presumed small. Alternatively, Eqn (5.2.14) can be

inverted numerically. This latter procedure was followed, since this

method converged very rapidly. Except at the smallest separations the

order of $\underset{\sim}{L}$ required for convergence was less than 20.

5.3 RESULTS

Before calculating any results, it is necessary to have some

idea of the magnitude of $1/\kappa$, the correlation length. For planar

surfaces, solutions of Eqns (5.1.3) and (5.1.5) give the following

result for the pressure P [6]:

$$P \simeq -4b\varepsilon_0^2 e^{-\kappa x} \qquad \kappa x \gg 1 .$$

Experimental data on lecithin bilayers is well described by an

exponential function with $1/\kappa \sim 1.9$ Å [6]. Since it is assumed that $1/\kappa$

is a constant independent of the nature of the interface, this value of

$1/\kappa$ will be used in the computations.

Let:

$$F_{12}(\kappa d) = b\varepsilon_0^2 V_0 F_{12}^*(\kappa d) ,$$

where V_0 is the volume of a water molecule. The quantity $[b\varepsilon_0^2 V_0] = E_B$ has a simple plysical interpretation. E_B represents the difference in energy between a water molecule at the interface and a water molecule in the bulk. In Fig. 5.1 the dimensionless solute-solute potential F_{12}^* is plotted as a function of d for several values of particle radii. The correlation length was taken to be $1/\kappa = 1.9$ Å, and $V_0 = 27$ Å^3.

Although a great deal of physical insight results from the very general expansion Eqn (5.1.1), it is now time to "pay the piper" for this generality. The parameter E_B will be different for different solute molecules, and there is apparently no *a priori* method of determining E_B. At first sight one might expect that comparison of the single sphere solution of Eqn (5.1.3) and solution energies would yield an estimate of E_B. However, since solute molecules will generally undergo some hydrogen bonding with water, the solvation energies will include the hydrogen bond energy. It is generally not possible to split up the solvation energy into "structural contributions" and "H-bond constributions".

However, methane is generally considered to undergo very little H-bonding in water. Unfortunately, the solvation energy of methane is not known experimentally. An estimate can be obtained from extrapolation of experimental data with more CH_2 groups. This gives a value of 3161 cal/mole [11], or $E_B = .77$ $k_B T$. From Fig. 5.1, the depth of the potential well (R = 2 Å) is ~ 1.6 $k_B T$ or ~ 1 kcal/mole. This compares with the result 1.4 kcal/mole from Monte Carlo calculations [14].

At this point it is worthwhile to recall the assumptions that have been made in this model:
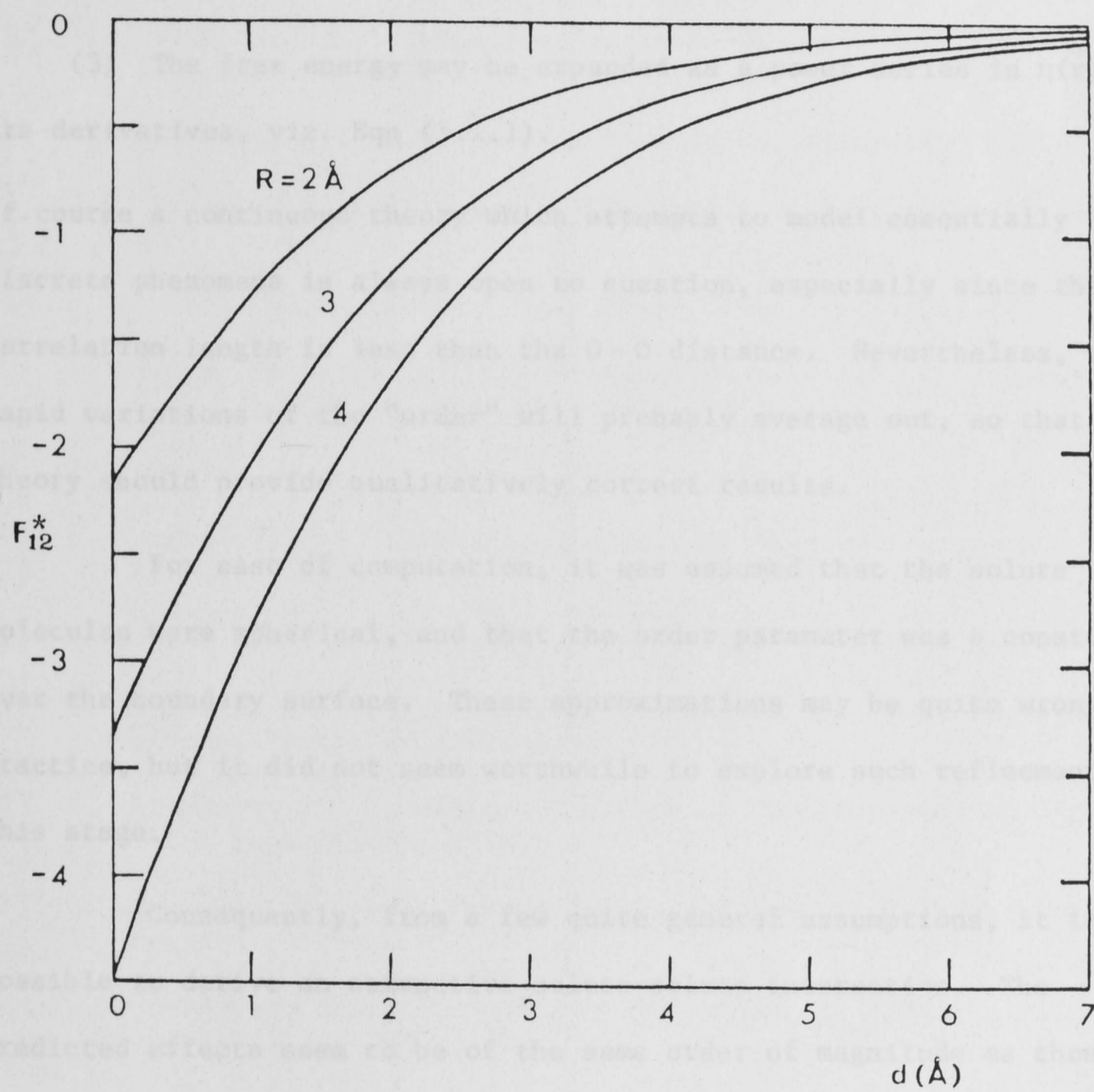
Fig. 5.1: The dimensionless solute-solute potential as a function of
separation d for various values of particle radii.

(1)   Water has a strong degree of angular correlation, resulting from tetrahedral co-ordination. The correlation manifests itself in a non-local response to a perturbation.

(2)   The structure of water may be described by an "order parameter" $\eta(\vec{r})$ which is a *continuous* function of position.

(3)   The free energy may be expanded as a power series in $\eta(\vec{r})$ and its derivatives, viz. Eqn (5.1.1).

Of course a continuous theory which attempts to model essentially discrete phenomena is always open to question, especially since the correlation length is less than the O - O distance. Nevertheless, these rapid variations of the "order" will probably average out, so that this theory should provide qualitatively correct results.

For ease of computation, it was assumed that the solute molecules were spherical, and that the order parameter was a constant over the boundary surface. These approximations may be quite wrong in practice, but it did not seem worthwhile to explore such refinements at this stage.

Consequently, from a few quite general assumptions, it is possible to derive an attractive solute-solute interaction. The predicted effects seem to be of the same order of magnitude as those obtained by Monte Carlo calculations.

REFERENCES — CHAPTER 5

[1] F. Franks, in *Water, A Comprehensive Treatise* (ed. F. Franks), Vol. V, Chap. 1 (Plenum Press: 1975).

[2] H.S. Franks and M.W. Evans, *J. Chem. Phys.* 13 (1945) 507.

[3] E.D. Finch and A.S. Schneider, *Biochim. Biophys. Acta* 406 (1975) 146, and the works cited therein.

[4] D.M. LeNeveu, R.P. Rand and V.A. Parsegian, *Nature* 259 (1976) 601.

[5] J.J. Kozak, W.S. Knight and W. Kauzmann, *J. Chem. Phys.* 48 (1968) 675.

[6] S. Marčelja and N. Radić, *Chem. Phys. Letts.* 42 (1976) 129.

[7] F. Franks, in *Water, A Comprehensive Treatise* (ed. F. Franks), Vol. IV, Chap. 1 (Plenum Press: 1975).

[8] J.A. Pople, *Proc. Roy. Soc.* A205 (1951) 163.

[9] L. Landau and E.M. Lifshitz, *Statistical Physics* (Pergamon, London: 1958).

[10] J.W. Cahn and J.E. Hilliard, *J. Chem. Phys.* 28 (1958) 258.

[11] S. Marčelja, D.J. Mitchell, B.W. Ninham and M.J. Sculley, *J.C.S., Faraday Trans. II* (in press).

[12] M. Abramowitz and I. Stegun, *Handbook of Mathematical Functions* (NBS, Washington: 1970).

[13] D. Langbein, *Theory of Van der Waals Attraction* (Springer-Verlag, Berlin: 1974).

[14] V.G. Dashevsky and G.N. Sarkisov, *Mol. Phys.* 27 (1974) 1271.

APPENDIX 1

In this appendix, the details of the calculations involved in determining the transition concentrations for the anisotropic fluid are given.

Let:

$$\beta^D = \sin\gamma + x + x|\cos\gamma| + \frac{4x}{\pi} E(\sin\gamma) + \frac{4}{\pi} x^2 \sin\gamma \qquad (A1.1)$$

$$\beta^R = \sin\gamma + x\ E(\sin\gamma) + \frac{\pi}{4} x|\cos\gamma| + \frac{\pi}{4} x + \frac{\pi}{4} x^2 \sin\gamma \ , \qquad (A1.2)$$

where

$$x = d/l \qquad \text{for rods}$$

$$= l/d \qquad \text{for discs} \ .$$

Eqn (2.3.2) can be written:

$$\frac{F}{Nk_BT} = \mu_0(T) + \log \rho_0 + \sigma + \frac{\lambda}{2} \Phi \ , \qquad (A1.3)$$

where

$$\sigma = \int f(\Omega)\ \log[4\pi f(\Omega)]\ d\Omega \qquad (A1.4)$$

$$\left.\begin{array}{l} \Phi = \displaystyle\iint \beta^D(\Omega,\Omega')\ f(\Omega)\ f(\Omega')\ d\Omega\ d\Omega' \quad \ldots \quad \text{discs} \\[1.5em] = \displaystyle\iint \beta^R(\Omega,\Omega')\ f(\Omega)\ f(\Omega')\ d\Omega\ d\Omega' \quad \ldots \quad \text{rods} \end{array}\right\} \qquad (A1.5)$$

$$\left.\begin{array}{l} \lambda = \dfrac{\pi}{2} \rho_0\ d^3 \quad \ldots \quad \text{discs} \\[1.5em] = 2l^2\ d\rho_0 \quad \ldots \quad \text{rods} \ . \end{array}\right\} \qquad (A1.6)$$

If σ and Φ depend on some parameter α, then the condition for minimization of the free energy is:

$$\sigma'(\alpha) + \frac{\lambda}{2} \Phi'(\alpha) = 0 . \tag{A1.7}$$

Note that when $x \to 0$, then $\beta^D \to \beta^R$, i.e. for very thin plates or rods, Eqn (A1.7) is formally identical for either rods or plates. The only difference is that λ has a different interpretation in each case. This correspondence was first noted by deGennes [1].

When the expansion for $f(\Omega)$, Eqn (2.3.4), is substituted into the expression for Φ, the following simple result is obtained:

$$\Phi = \sum_{N=0,2,4,\ldots} (2\pi)^2 \frac{a_N^2 c_N}{(N+\frac{1}{2})} ,$$

where

$$c_N = \int_0^\pi \beta(\gamma) \, \rho_N(\cos\gamma) \, \sin\gamma \, d\gamma .$$

The unsuperscripted $\beta(\gamma)$ refers to β^D or β^R, whichever is appropriate. Unfortunately, because of the highly non-linear nature of σ, no corresponding simplification is possible with this term.

For given λ, the a_i are determined by numerical minimization of Eqn (A1.3) [2]. Bearing in mind Eqn (A1.7), the chemical potential and osmotic pressure in the ordered (anisotropic) phase are given by:

$$\mu_a = k_B T[\mu_0 + 1 + \log \rho_a + \sigma_a + \lambda_a \Phi_a]$$

$$P_a = k_B T\left(\rho_a + \frac{\lambda_a \rho_a}{2} \Phi_a\right) , \tag{A1.8}$$

where σ_a and Φ_a are the values of σ and ϕ in the anisotropic phase. The corresponding expressions for the isotropic phase are:

$$\mu_I \;=\; k_B T [\mu_0 + \log \rho_I + \rho_I \lambda_I]$$

$$P_I \;=\; k_B T \left(\rho_I + \frac{\lambda_I}{2} \, \rho_I \Phi_I \right) . \tag{A1.9}$$

Here Φ_I is given simply by:

$$\Phi_I \;=\; \frac{\pi}{4} + \left(\frac{\pi+3}{2} \right) x + x^2 \qquad \cdots \qquad \text{discs}$$

$$=\; \frac{\pi}{4} \left\{ 1 + \left(\frac{\pi+3}{2} \right) x + \frac{\pi}{4} x^2 \right\} \qquad \cdots \qquad \text{rods} .$$

The transition concentrations of the two phases, and hence the pressures can be determined by equating Eqn (A1.8) and Eqn (A1.9) viz.:

$$\log \lambda_I + \lambda_I \Phi_I \;=\; \log \lambda_a + \sigma_a + \lambda_a \Phi_a$$

$$\lambda_I + \frac{\lambda_I^2}{2} \Phi_I \;=\; \lambda_a + \frac{\lambda_a^2}{2} \Phi_a .$$

These equations were solved to give the results shown in Chapter 2.

APPENDIX 2

The free energy, Eqn (4.4.1), is expressed in a form suitable for computation in the following. From Eqn (4.2.5)

$$e \int_0^{\psi_0} \Gamma(\psi_0') \, d\psi_0' = \left(\frac{n_+ \, \varepsilon \, k_B T}{2\pi} \right)^{\frac{1}{2}} \int_0^{\psi_0} \left(e^{-e\psi_0'/k_B T} + (1 + 2c_1) \, e^{+e\psi_0'/k_B T} \right.$$

$$\left. + c_1 \, e^{-e\psi_0'/k_B T} - (2 + 3c_1) \right)^{\frac{1}{2}} d\psi_0'$$

$$= \frac{k_B T}{e} \left(\frac{n_+ \, \varepsilon \, k_B T}{2\pi} \right)^{\frac{1}{2}} \int_1^{e^{e\psi_0/k_B T}} \sqrt{F(u)} \, \frac{du}{u^2} \, , \qquad (A2.1)$$

where

$$F(u) = (1 + 2c_1) u^3 - (2 + 3c_1) u^2 + u + c_1 \ .$$

Consequently the energy per particle g, can be written as:

$$\frac{g}{k_B T} = z^* \int_1^u \sqrt{F(u')} \, \frac{du'}{(u')^2}$$

$$+ \, x \log x + (1 - x) \, \log(1 - x) + x \, \log\left(\frac{x - y}{x} \right) \, , \qquad (A2.2)$$

where

$$x = \frac{\Gamma_A}{\Gamma_A + \Gamma_B} \qquad\qquad y = \frac{\Gamma}{\Gamma_A + \Gamma_B}$$

$$z^* = \left(\frac{n_+ \, \varepsilon \, k_B T}{2\pi} \right)^{\frac{1}{2}} \frac{1}{e(\Gamma_A + \Gamma_B)} \qquad u = e^{e\psi_0/k_B T} \ .$$

The integral in Eqn (A2.1) can be evaluated in terms of elliptic

functions (see Appendix 3). The values of y and u are determined from

the solutions of the transcendental equations:

$$\frac{yu^{-1}}{x - y} = 10^{pH - pK}$$

$$y = z^*[u^{-1} + (1 + 2c_1)u + c_1u^{-2} - (2 + 3c_1)]^{\frac{1}{2}} .$$

The solutions of these equations were substituted into Eqn (A2.2), to

give the results shown in Fig. 4.2 and Fig. 4.3.

APPENDIX 3

In this appendix, the integral in Eqn (A2.1) is expressed in terms of elliptic functions. Unless explicitly stated otherwise, all properties of elliptic integrals and theta functions used in the following derivations can be found in refs. [3,4].

The integral in Eqn (A2.1) can be written as:

$$I = \int_1^u \frac{F(u') \, du'}{(u')^2 \, \sqrt{F(u')}}$$

$$F(u') = (1 + 2c_1)u^3 - u^2(2 + 3c_1) + u + c_1 .$$

(A3.1)

As is well known, any integral of the form:

$$\int R(w,x) \, dx ,$$

where R is the rational function of w and x, w^2 being a quartic or cubic function in x, can be expressed in terms of elliptic integrals. Eqn (A3.1) can be reduced to the standard form:

$$I = \frac{3}{2}(1 + 2c_1)I_1 - (2 + 3c_1)I_0 + \frac{I_{-1}}{2} - \frac{\sqrt{F}}{u}$$

(A3.2)

$$I_1 = \int \frac{u}{\sqrt{F}} \, du \qquad I_0 = \int \frac{du}{\sqrt{F}} \qquad I_{-1} = \int \frac{du}{u\sqrt{F}} .$$

The above can be derived by integrating both sides of $d/dx(\sqrt{F}/x)$. The function $F(u)$ can be factored as follows:

$$F = (u-1)(u-u^+)(u-u^-) ,$$

where

$$u^{\pm} = \frac{(1+c_1) \pm \sqrt{(1+c_1)^2 + 4c_1(1+2c_1)}}{1+2c_1} .$$

Since $c_1 < 1$, $u^+ > 0$, $u^- < 0$. Substituting $u = (1-u^-)t^2 + u^-$ into $du/\sqrt{F}$ yields:

$$\int_1^{e^{e\psi_0/k_B T}} \{u\} \frac{du}{\sqrt{F}} = Q \int_1^w \{u\} \frac{dt}{[(1-k^2t^2)(1-t^2)]^{\frac{1}{2}}}$$

$$k^2 = \frac{1-u^-}{u^+ - u^-} \qquad w = \left(\frac{e^{e\psi_0/k_B T} - u^-}{1-u^-} \right)$$

$$Q = \frac{2}{[(u^+ - u^-)(1+2c_1)]^{\frac{1}{2}}} ,$$

where $\{u\}$ represents $u, 1, u^{-1}$. Note that since $\psi < 0$, $w < 1$, so that all these integrals are negative.

Using the following properties of elliptic functions:

$$\frac{d}{dv} snv = cnv \; dnv \qquad sn^2v + cn^2v = 1$$

$$k^2 \; sn^2v + dn^2v = 1$$

and the substitution $t = snv$, I_0 becomes:

$$I_0 = Q[sn^{-1}w + K] .$$

Here K is the complete elliptic integral of the first kind. Using a similar substitution, I_{+1} can be reduced to:

$$I_{+1} = u^- I_0 + Q(1-u^-)[E - E(sn^{-1}w)] ,$$

where E is the complete elliptic integral of the second kind, and

$E(sn^{-1}w)$ is the incomplete elliptic integral of the second kind.

I_{-1} can be reduced to:

$$I_{-1} = \frac{Q}{u^-} I'_{-1} ,$$

where

$$n = \frac{1 - u^-}{u^-} \qquad I'_{-1} = \int_1^w \frac{dt}{(1 + nt^2)[(1 - k^2 t^2)(1 - t^2)]^{\frac{1}{2}}} . \qquad (A3.3)$$

This can be expanded directly in terms of Jacobian theta functions [5]:

$$I'_{-1} = \frac{1}{2} \log\left(\frac{\theta_1\left(\frac{(\gamma + p)\pi}{2K}\right)}{\theta_1\left(\frac{(\gamma - p)\pi}{2K}\right)}\right) + \frac{(K - p)A}{2K} \frac{\theta'_4\left(\frac{\gamma\pi}{2K}\right)}{\theta_4\left(\frac{\gamma\pi}{2K}\right)}$$

$$p = sn^{-1}w \qquad \gamma = sn^{-1}\sqrt{-1/n} \qquad A = \frac{sn\gamma}{cn\gamma \ dn\gamma} .$$

θ_4 is the usual notation for the 4th theta function. The prime denotes differentiation with respect to the argument.

The various elliptic integrals can be expressed in terms of theta functions, which in turn can be given in terms of the nome q:

$$q = \Delta + 2\Delta^5 + 15\Delta^9 + \ldots ,$$

where:

$$\Delta = \frac{1}{2}\left(\frac{1 - \sqrt{k'}}{1 + \sqrt{k'}}\right)$$

$$(k')^2 = 1 - k^2 .$$

The following series expansions are given in many texts [3,4]:

$$K = \frac{\pi}{2} + 2\pi \sum_{s=1}^{\infty} \frac{q^s}{1 + q^{2s}}$$

$$\frac{E}{K} = \frac{2 - k^2}{3} + \frac{\pi^2}{k^2}\left(\frac{1}{12} - 2\sum_{s=1}^{\infty} \frac{q^{2s}}{(1 - q^{2s})^2}\right)$$

$$snz = \frac{2\pi}{kK} \sum_{N=0}^{\infty} \frac{q^{N+\frac{1}{2}}}{(1-q^{2N+1})} \sin\left((2N+1)\frac{\pi z}{2K}\right)$$

$$\frac{\pi}{2K} \frac{\theta_4'\left(\frac{\gamma\pi}{2K}\right)}{\theta_4\left(\frac{\gamma\pi}{2K}\right)} = \frac{2\pi}{K} \sum_{N=1}^{\infty} \frac{q^N \sin\left(\frac{N\gamma\pi}{K}\right)}{1-q^{2N}}$$

and [5]

$$\frac{1}{2} \log \frac{\theta_1\left(\frac{[\gamma+u]\pi}{2K}\right)}{\theta_1\left(\frac{[\gamma-u]\pi}{2K}\right)}$$

$$= \frac{1}{2} \log \frac{\sin\left(\frac{[\gamma+u]\pi}{2K}\right)}{\sin\left(\frac{[\gamma-u]\pi}{2K}\right)} + 2 \sum_{N=1}^{\infty} \frac{1}{N} \left(\frac{q^{2N}}{1-q^{2N}}\right) \sin\left(\frac{N\gamma\pi}{K}\right) \sin\left(\frac{Nu\pi}{K}\right).$$

Since $q \lesssim .1$, for c_1 in the range $0-1$, the first five terms of the above series are adequate for numerical purposes.

REFERENCES — APPENDICES 1 - 3

[1] P.G. deGennes, *The Physics of Liquid Crystals* (Clarendon Press, Oxford: 1974).

[2] M.R. Osborne and M.A. Saunders, in *Descent Methods in Optimization* (eds. Anderssen, Jennings and Ryan), (University of Queensland Press: 1972).

[3] M. Abramowitz and I. Stegun, *Handbook of Mathematical Functions* (NBS, Washington: 1970).

[4] E.T. Whittaker and G.N. Watson, *A Course in Modern Analysis* (Cambridge University Press: 1965).

[5] F.G. Tricomi, *Elliptische Funktionen* (Akemische Verlagsgesellschaft, Leipzig: 1948).